Available online at www.sciencedirect.com

ScienceDirect

Nuclear Physics B 896 (2015) 412–439

NUCLEAR PHYSICS B

www.elsevier.com/locate/nuclphysb

Phenomenology of baryogenesis from lepton-doublet mixing

Björn Garbrecht [a,*], Ignacio Izaguirre [a,b]

[a] *Physik Department T70, James-Franck-Straße, Technische Universität München, 85748 Garching, Germany*
[b] *Max-Planck-Institut für Physik (Werner-Heisenberg-Institut), Föhringer Ring 6, 80805 München, Germany*

Received 3 December 2014; received in revised form 17 April 2015; accepted 20 April 2015

Available online 23 April 2015

Editor: Tommy Ohlsson

Abstract

Mixing lepton doublets of the Standard Model can lead to lepton flavour asymmetries in the Early Universe. We present a diagrammatic representation of this recently identified source of *CP* violation and elaborate in detail on the correlations between the lepton flavours at different temperatures. For a model where two sterile right-handed neutrinos generate the light neutrino masses through the see-saw mechanism, the lower bound on reheat temperatures in accordance with the observed baryon asymmetry turns out to be $\gtrsim 1.2 \times 10^9$ GeV. With three right-handed neutrinos, substantially smaller values are viable. This requires however a tuning of the Yukawa couplings, such that there are cancellations between the individual contributions to the masses of the light neutrinos.

1. Introduction

Observational and theoretical studies of mixing and oscillations are typically concerned with neutral particle states. Important examples are neutral meson mixing, the oscillations of Standard Model (SM) neutrinos [1] and Leptogenesis through the mixing of sterile right-handed neutrinos (RHNs) in the early Universe [2–5]. In contrast, for charged particles in the SM at vanishing temperature, mass degeneracies between different states are not strong enough to produce observable

* Corresponding author.
E-mail address: garbrecht@tum.de (B. Garbrecht).

http://dx.doi.org/10.1016/j.nuclphysb.2015.04.017

phenomena of mixing and oscillations. This does however not preclude the fact that these effects are present in principle. Moreover, it has been demonstrated that the mixing of lepton doublets (which are gauged) can be of importance for Leptogenesis [6–10]: At high temperatures, the asymmetries are in general produced as superpositions of the lepton doublet flavour eigenstates of the SM. In the SM flavour basis, this can be described in terms of off-diagonal correlations in the two-point functions, or alternatively in effective density-matrix formulations in terms of correlations of charge densities of different flavours. At smaller temperatures, interactions mediated by SM Yukawa couplings become faster than the Hubble expansion, such that the flavour correlations decohere. In particular, the SM leptons receive thermal mass corrections as well as damping rates that lift the flavour degeneracy. By now, these effects have been investigated in detail. It turns out that due to the interplay with gauge interactions, the flavour oscillations that may be anticipated from the thermal masses are effectively frozen, while the decoherence proceeds mainly through the damping effects, *i.e.* the production and the decay of leptons in the plasma [9,10]. The appropriate treatment of these flavour correlations turns out to be of leading importance for the washout of the asymmetries from the out-of-equilibrium decays and inverse decays of the RHNs.

The origin of the charge–parity (*CP*) asymmetry for Leptogenesis is usually attributed to the RHNs and their couplings [11]. In the standard calculation, when describing the production and the decay of the RHNs through *S*-matrix elements, one can diagrammatically distinguish between vertex and wave-function terms. The presence of finite-temperature effects as well as the notorious problem of correctly counting real intermediate states in the Boltzmann equations [12] have motivated the use of techniques other than the *S*-matrix approach: It has been demonstrated that the wave-function contribution can alternatively be calculated by solving kinetic equations (that are Kadanoff–Baym type equations which descend from Schwinger–Dyson equations, see Refs. [13–17] on the underlying formalism) for the RHNs and their correlations, or equivalently, by solving for the evolution of their density matrix [18–25]. The vertex contributions to the decay asymmetry can be obtained within the Kadanoff–Baym framework as well, as it is shown in Refs. [26–32]. We note at this point that it has more recently been argued that the asymmetry from the wave-function correction and the contribution from the kinetic equation are distinct contributions that should be added together [33,34]. However, it is shown in Refs. [19–21] that the kinetic equations derived from the two-particle irreducible effective action capture all contributions of relevance for the *CP* asymmetry at leading order, which also encompasses the wave-function corrections.

The calculations for Leptogenesis based on Schwinger–Dyson equations on the Closed-Time-Path (CTP) can also be applied to Leptogenesis from oscillations of light (masses much below the temperature) RHNs [35], also known as the ARS scenario after the authors of Ref. [36]. In this approach, we can interpret the *CP* violation as originating from cuts of the one-loop self-energy of the RHNs, that are dominantly thermal. It can be concluded that thermal effects can largely open the phase–space for *CP*-violating cuts that are strongly suppressed for kinematic reasons at vanishing temperature.

Putting together the elements of flavour correlations for charged particles and of thermal cuts, we can identify new sources for the lepton asymmetry, in addition to the one from cuts in the RHN propagator. In models with multiple Higgs doublets, Higgs bosons may be the mixing particles [37], whereas in minimal type-I see-saw scenarios (with one Higgs doublet), this role can be played by mixing SM lepton doublets [38]. Yet, the RHNs remain of pivotal importance because due to their weak coupling, they provide the deviation from thermal equilibrium that is necessary for any scenario of baryogenesis.

While the set of free parameters of the type-I see-saw model will remain underconstrained by present observations and those of the foreseeable future, the parameter space in that scenario is still much smaller than in models with multiple Higgs doublets. For our phenomenological study, we therefore choose to consider the mixing of lepton doublets in the see-saw scenario, that is given by the Lagrangian

$$\begin{aligned}\mathcal{L} = {} & \frac{1}{2}\bar{N}_i(\mathrm{i}\partial\!\!\!/\delta_{ij} - M_{Nij})N_j + \bar{\ell}_a \mathrm{i}\partial\!\!\!/\ell_a + (\partial^\mu\phi^\dagger)(\partial_\mu\phi) \\ & - Y^*_{ia}\bar{\ell}_a\tilde{\phi}P_{\mathrm{R}}N_i - Y_{ia}\bar{N}_i P_{\mathrm{L}}\tilde{\phi}^\dagger\ell_a - h_{ab}\phi^\dagger\bar{e}_{\mathrm{R}a}P_{\mathrm{L}}\ell_b - h^*_{ab}\phi\bar{\ell}_b P_{\mathrm{R}}e_{\mathrm{R}_a}\,. \end{aligned} \tag{1}$$

In short, the scenario of baryogenesis from mixing lepton doublets can be described as follows [38]: Flavour-off diagonal correlations from the mixing of active leptons ℓ_a (where a is the flavour index) can induce the production of lepton flavour asymmetries, corresponding to diagonal entries of a traceless charge density matrix in flavour space. Different washout rates for the particular flavours may then lead to a net asymmetry in total lepton number, *i.e.*, a non-vanishing trace of the charge density matrix. Now, since off-diagonal correlations due to mixing vanish in thermal equilibrium, the mixing of lepton doublets that we aim to describe consequently is an out-of-equilibrium phenomenon. It is thus natural to assume that initially, when the primordial plasma is close to thermal equilibrium, all correlations between the SM lepton flavours vanish. Therefore, we are interested in possibilities of generating these dynamically. Due to gauge interactions, the distribution functions of the SM particles should track their equilibrium forms very closely. Moreover, gauge interactions are flavour-blind, so they can neither generate flavour correlations nor destroy these (up to the indirect effects that we discuss below). Sizeable off-diagonal correlations can however be induced through couplings to the RHNs N, the distributions of which can substantially deviate from equilibrium. The flavour correlations in the doublet leptons ℓ are suppressed however due to the SM Yukawa couplings h with the charged singlets e_{R} and the Higgs field ϕ, where $\tilde{\phi} = (\epsilon\phi)^\dagger$, and where ϵ is the totally antisymmetric SU(2) tensor. By field redefinitions, we can impose that h and M_N are diagonal, which is a common and convenient choice of basis that we adapt throughout this present paper. For simplicity, we therefore write $M_{Ni} \equiv M_{Nii}$.

In this paper, within Section 2, we first review the scenario of Ref. [38]. We improve on the previous discussion by introducing a diagrammatic representation of the mechanism. Moreover, we carefully discuss the generation and the decoherence of lepton flavour correlations at different temperatures, paying particular attention to the fact that both effects take a finite time to fully establish. Section 3 contains a survey of the parameter space of baryogenesis from mixing lepton doublets based on the Lagrangian (1). Under the assumption that only two RHNs are present, we perform a comprehensive scan, given the present best-fit values on the light neutrino mass differences and mixing angles, such that we can identify the point in parameter space that allows for the lowest reheat temperature for which an asymmetry in accordance with observation can result. In addition, we show that for three RHNs, substantially smaller temperatures can be viable, what requires however anomalously large Yukawa couplings of the μ- and the τ-leptons and a cancellation in their contributions to the mass matrix of the light neutrinos. The analysis is however restricted to the strong washout regime, such that it remains an open question of interest whether favourable parametric regions also exist when at least one of the RHNs induces only a weak washout. The concluding remarks are given in Section 4.

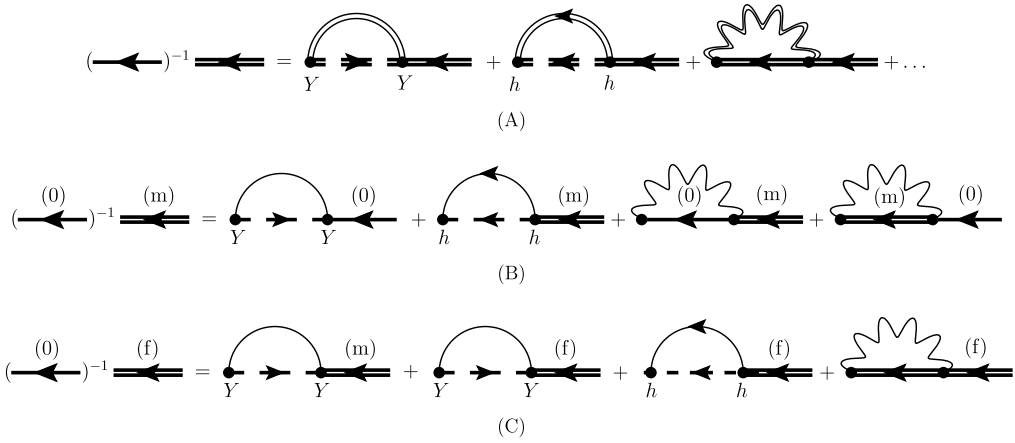

Fig. 1. The diagrams (A) are a graphical representation of the Kadanoff–Baym equations that account for the lepton–Yukawa interactions h and Y as well as gauge interactions. Single lines stand for tree-level propagators and double lines for full propagators. Bold solid lines with an arrow are propagators of the SM lepton doublets ℓ, and dashed bold lines with an arrow of the Higgs doublet ϕ. Regular solid lines with an arrow are propagators for the right-handed SM leptons e_{R}, regular solid lines without an arrow stand for the RHNs N and wiggly lines for SM gauge bosons. The dots ... indicate extra diagrams of different topology than those drawn explicitly and that can be derived from the 2-particle irreducible effective action. Figures (B) and (C), illustrate the scheme that is used in Ref. [38] to obtain approximate solutions, which we also apply in this work. The full propagators for the doublets ℓ are now approximated by the results including flavour correlations. The loops are understood to include gauge-mediated processes and top loops that open up the phase space for the reactions between the particles, that are approximated to be massless, *cf. e.g.* Ref. [44]. The superscripts $(0, \mathrm{m}, \mathrm{f})$ indicate that the charge density matrix that can be computed from the corresponding propagators for ℓ yields the non-zero entries of $q_{\ell}^{(0,\mathrm{m},\mathrm{f})}$.

2. Generation and freeze-out of the lepton asymmetry

2.1. Diagrammatic representation of the CP-violating source terms

A detailed derivation of the source term for the asymmetries of the individual lepton flavours is presented in Ref. [38], where the CTP method is employed. Here, we do not reiterate these technical details, but we explain the qualitative form of the main results with the help of a diagrammatic representation of the Kadanoff–Baym equations that arise from the CTP approach. In particular, we express the perturbative approximations to the solutions of these equations diagrammatically. Moreover, we discuss how the mixing of the SM lepton doublets in the CTP formalism can be related to a density matrix formulation of flavour oscillations, that should be familiar *e.g.* from the problem of oscillations of active neutrinos [39–43].

The CTP formulation of the problem leads to Kadanoff–Baym equations, that we show here in a diagrammatic form in Fig. 1(A). One may interpret the Kadanoff–Baym equations as (a subset of) exact Schwinger–Dyson equations, that can only be solved approximately in practice. Since couplings can be assumed to be weak, a perturbative one-loop expansion, that is indicated by Figs. 1(B) and (C), amounts to a valid approximation.

We can assume that kinetic equilibrium is established by fast gauge interactions. The distribution functions and the propagators of the SM leptons ℓ are therefore effectively determined by the matrix $q_{\ell ab}$ of the charge densities of ℓ and their flavour correlations [9]. The perturbation expansion then explicitly reads $q_{\ell} = q_{\ell}^{(0)} + q_{\ell}^{(\mathrm{m})} + q_{\ell}^{(\mathrm{f})} + \cdots$, where the superscript (m) stands

for mixing and (f) for flavoured asymmetries. The zeroth order term is given by the equilibrium distribution for a vanishing charge density, and therefore $q_\ell^{(0)} = 0$. The contributions $q_\ell^{(\mathrm{m})}$ and $q_\ell^{(\mathrm{f})}$ are induced by the non-equilibrium right-handed neutrinos and are discussed in the following Subsections.

In order to clarify the relation of the present notation with the one used in the derivation of Ref. [38], we make the following remarks: In the present context, the interesting contributions within $q_\ell^{(\mathrm{m})}$ are the off-diagonal correlations of lepton doublets, as these are referred to in Ref. [38]. The leading *CP*-violating lepton-flavour asymmetries are then contained in $q_\ell^{(\mathrm{f})}$. Note also that the first term on the right-hand side of the equation in Fig. 1(C) is called the source term in Ref. [38].

One should notice that when deriving the kinetic equations from the two-particle irreducible effective action, the leading *CP*-violating contributions arising from wave-function corrections only involve one-loop diagrams at the level of Kadanoff–Baym equations, which are however expressed in terms of resummed propagators [19]. For standard Leptogenesis sufficiently far away from the mass-degenerate regime, the resummed propagators can be expanded such that the leading *CP*-violating self-energy exhibits the familiar two-loop form in terms of tree-level propagators [30]. In the extremely mass-degenerate case, when the mass-splitting of the RHNs becomes comparable to their width, such an expansion is no longer possible and instead, solving the Kadanoff–Baym equations in terms of resummed propagators and one-loop diagrams appears to be the only presently viable technique to obtain solutions [20,22–24] because the mass-splitting of the active leptons is induced by their thermal masses that are by construction of a size comparable to their thermal width, we should use the approach based on resummed propagators, as diagrammatically indicated by Fig. 1(A). As specified in Ref. [38], when we integrate these Kadanaoff–Baym equations over four momentum, we obtain density-matrix type equations for the number densities of leptons and anti-leptons as well as their flavour correlations, that we discuss in the following.

2.1.1. Equations for mixing correlations

The first order approximation to the Kadanoff–Baym equations, that is given in Fig. 1(B), has the main qualitative features of a density-matrix equation

$$\partial_t \varrho + \mathrm{i}[M, \varrho] = \Theta - \frac{1}{2}\{\Gamma, \varrho\}\,, \tag{2}$$

where t denotes time, M is a mass matrix, Γ a matrix that describes relaxation toward equilibrium and Θ a matrix-valued inhomogeneous term. This equation is of a form that is familiar from many applications, among which are neutrino oscillations [39–43] and ARS Leptogenesis [20, 36,45–49]. In particular, it is the commutator term $[M, \varrho]$ that induces flavour oscillations among the off-diagonal components of ϱ.

Now for the present application, we replace the density matrix ρ by the deviations of the lepton and anti-lepton number densities from their equilibrium values $\delta n_\ell^{\pm(\mathrm{m})}$. Qualitative remarks on the relation and the practical advantages of our expansions and approximations compared to fully flavour-covariant formulations that may be derived in the CTP or a density-matrix framework are given in Section 2.1.4. The off-diagonal components of $\delta n_\ell^{\pm(\mathrm{m})}$ describe the flavour correlations of these non-equilibrium densities. The matrices $\delta n_\ell^{\pm(\mathrm{m})}$ then evolve according to the following equations [38]:

$$\frac{27\zeta(3)T_{\rm com}}{\pi^2}\partial_\eta \delta n^{\pm({\rm m})}_{\ell ab} \pm {\rm i}\frac{\left(h^2_{aa}-h^2_{bb}\right)T^2_{\rm com}}{16}\delta n^{\pm({\rm m})}_{\ell ab}$$
$$= -\sum_i Y^\dagger_{ai}Y_{ib}B^Y_i - (h^2_{aa}+h^2_{bb})B^{\rm fl}_\ell \delta n^{\pm({\rm m})}_{\ell ab} - B^g_\ell(\delta n^{+({\rm m})}_{\ell ab}+\delta n^{-({\rm m})}_{\ell ab})\,. \tag{3}$$

Here, η is the conformal time, which is suitable for performing calculations in the background of the expanding Universe. It is determined up to redefinitions of the scale factor, and we make the choice that the physical temperature in the radiation-dominated Universe is $T = 1/\eta$, what determines the comoving temperature used in above equations to be

$$T_{\rm com} = \frac{m_{\rm Pl}}{2}\sqrt{\frac{45}{\pi^3 g_\star}}\,, \tag{4}$$

where $m_{\rm Pl}$ is the Planck mass and $g_\star$ the number of relativistic degrees of freedom. Eqs. (3) are derived in Ref. [38] by integrating the corresponding Kadanoff–Baym equations for distribution functions of lepton and antileptons and their flavour correlations over the spatial momentum $\mathbf{p}$, and they are given diagrammatically in Fig. 1(B). For the distribution functions, we have assumed that gauge interactions maintain these to be of the Fermi–Dirac form with a matrix-valued chemical potential, as explained in Ref. [9]. This allows to uniquely relate the momentum-space distributions to the number densities δn_ℓ in Eq. (3).

We now give explaining remarks on the individual terms in Eqs. (3):

- The terms $\propto (h^2_{aa}-h^2_{bb})$ are present due to thermal masses and correspond to the commutator term in the density-matrix equation (2). Notice the different sign of these terms in the equations for lepton and anti-lepton densities, that was first noted in Ref. [9]. This is what makes it necessary to treat the lepton and anti-lepton densities differently, rather than considering the matrix of charge densities and their and correlations $q^{({\rm m})}_\ell = \delta n^{+({\rm m})}_\ell - \delta n^{-({\rm m})}_\ell$.
- The terms involving B^Y_i describe the decays and inverse decays of sterile neutrinos into the active leptons. Provided the distribution of the sterile neutrinos N deviates from thermal equilibrium, these processes induce the flavour correlations of active leptons through the off-diagonal components ($a \neq b$) of $Y^\dagger_{ai}Y_{ib}$ in first place. In this work, we restrict ourselves to the parametric regime where the freeze-out value of the lepton asymmetry is determined at times when the distribution of the N_i is dominated by non-relativistic particles, commonly referred to as strong washout. For this situation, we can assume that $M_{Ni} \gg T$, and approximate the rate for decays and inverse decays using [38]

$$B^Y_i \approx -\frac{T^{\frac{3}{2}}M^{\frac{7}{2}}_{Ni}}{2^{\frac{13}{2}}\pi^{\frac{5}{2}}}\frac{\mu_{Ni}}{T}{\rm e}^{-\frac{M_{Ni}}{T}}\,. \tag{5}$$

  Here, μ_{Ni} denotes a pseudochemical potential that can be employed in order to describe the deviation

$$\delta f_{Ni}(\mathbf{p}) = f_{Ni}(\mathbf{p}) - f^{\rm eq}_{Ni}(\mathbf{p}) \approx \frac{\mu_{Ni}}{T}{\rm e}^{\sqrt{\mathbf{p}^2+M^2_{Ni}}/T} \tag{6}$$

  of f_{Ni}, which is the distribution function of the sterile neutrino N_i, from its equilibrium form $f^{\rm eq}_{Ni}$. For standard Leptogenesis, results for the lepton asymmetry obtained when using a distribution function numerically derived from the Boltzmann equations before momentum-averaging are compared to the results obtained when using the approximation with a pseudochemical potential in Refs. [30,50], and the discrepancy between the two methods is found

to be small because for strong washout, the RHNs are non-relativistic, such that they mostly populate modes with momenta that are small compared to the temperature. Within the density-matrix equation (2), the B_i^Y terms correspond to the inhomogeneous term Θ. In the diagrammatic equation Fig. 1(B), this is the first term on the right-hand side.
Note also that since the factor B_i^Y mediates the creation of off-diagonal flavour correlations and CP-violation in Eq. (3), it comprises an absorptive cut contribution. Since the leptons are rapidly redistributed due to gauge interaction, by the use of quantities such as B_i^Y, that are readily convoluted with the lepton-distribution functions in kinetic equilibrium, we avoid the notation of recurring integrals. The relation to the cut-contribution to the lepton self-energy is explained in Appendix A.

- The terms with $B_\ell^{\not{\mathrm{fl}}}$ describe the decay of the flavour correlations due to the SM Yukawa interactions, that discriminate between the different lepton flavours. In the density-matrix equation (2), they correspond to the anticommutator term involving the relaxation rate Γ, and in Fig. 1(B) to the second term on the right-hand side. The relevant processes involve the radiation of extra gauge bosons or the decay and inverse decay of a virtual Higgs boson into a pair of top quarks, which are understood to be contained in the loops. (Otherwise, the $1 \leftrightarrow 2$ processes between approximately massless particles would be strongly suppressed kinematically.) The rates for these processes are calculated to LO in Ref. [44], where it is found that $\gamma^{\not{\mathrm{fl}}} = 5 \times 10^{-3}$ (see also Ref. [51] for an earlier estimate that leads to a similar quantitative conclusion and Refs. [52,53] for a recent LO calculation for the production of massless sterile neutrinos, that is closely related). Taking the momentum average of the kinetic equations of Ref. [38], we find that $B_\ell^{\not{\mathrm{fl}}} = 54\zeta(3)/\pi^2 \times \gamma^{\not{\mathrm{fl}}} T \approx 3.3 \times 10^{-2} T^2$, what differs from the value used in Ref. [38] due to the updated result of Ref. [44]. We note that the averaging implies the assumption that flavour correlations in all momentum modes decay at the same rate, which is not the case in reality. This procedure should therefore incur an order one inaccuracy that may be removed in the future by extra numerical efforts.
- Finally, the contribution with B_ℓ^g describes pair creation and annihilation processes that drive $\delta n_{ab}^+ + \delta n_{ab}^-$ toward zero. It thus forces an alignment between the correlations among the different flavours of leptons and of anti-leptons, that would otherwise perform oscillations with opposite angular frequency, and as a consequence, the evolution of the off-diagonal correlations is overdamped [9,10]. Gauge interactions thus contribute indirectly to the decay of flavour correlations in addition to the direct damping through the Yukawa interactions. In Ref. [38], the relevant momentum average of the pair creation and annihilation rate is estimated as $B_\ell^g = 1.7 \times 10^{-3} T^2$, based on the thermal rates for s-channel mediated processes, that should yield the dominant contribution due to the large number of degrees of freedom in the SM.

Ignoring the derivative with respect to the conformal time η, the solution to Eqs. (3) is given by

$$q_{\ell ab}^{(\mathrm{m})} = \delta n_{\ell ab}^{+(\mathrm{m})} - \delta n_{\ell ab}^{-(\mathrm{m})} = \mathrm{i}\Xi_{ab}(\mathcal{Q}_{\ell ab}/T^2) \sum_i Y_{ai}^\dagger Y_{ib} B_i^Y \,, \tag{7}$$

where

$$\mathcal{Q}_{\ell ab} = \frac{(h_{aa}^2 - h_{bb}^2)(T^4/8)}{\left[(h_{aa}^2 - h_{bb}^2)/16\right]^2 T^4 + (h_{aa}^2 + h_{bb}^2) B^{\not{\mathrm{fl}}} [2B_\ell^g + (h_{aa}^2 + h_{bb}^2) B_\ell^{\not{\mathrm{fl}}}]} \tag{8}$$

and where Ξ is a matrix specified in Eq. (14) below, that selects only those correlations that have enough time to be built up at the temperatures of interest. The flavour matrix $\mathcal{Q}_\ell$ can be viewed as the quantity that multiplies the *CP*-violation originating from the Yukawa couplings Y of the sterile neutrinos. By comparing the powers of h in the numerator and the denominator, we explicitly see that the $q^{(\mathrm{m})}_{\ell ab}$ become suppressed if h_{aa} or h_{bb} become large. This is because processes mediated the SM lepton Yukawa interactions lead to decoherence these off-diagonal correlations, as it is familiar from flavoured Leptogenesis [7–9]. Note that these decoherence effects also avoid the resonance catastrophe that would occur for $h_{aa} \to h_{bb}$ in their absence.

Neglecting the time derivatives is justified provided that there is enough time for the flavour correlations to adapt to the change in the non-equilibrium density of the sterile neutrinos. From Eqs. (3), it can be seen that rate for the flavour correlations to build up is given by

$$\Gamma^{-}_{q_{\ell ab}} = \frac{\pi^2}{54\zeta(3)T}\left(B^g_\ell + (h^2_{aa}+h^2_{bb})B^{\not g}_\ell - \sqrt{B^{g\,2}_\ell - \left[(h^2_{aa}-h^2_{bb})T^2/16\right]^2}\right). \tag{9}$$

This implies that the correlations do not build up in case the entries of h are so small that $\Gamma^{-}_{q_{\ell ab}} \lesssim H$ when the right-handed neutrinos go out of equilibrium. One should expect this, because in the limit $h \to 0$, the system is flavour blind and there should be no dynamical generation of correlations. For the subsequent discussion, it is useful to compare the rate for the build up of correlations (9) with the more commonly employed rate of flavour equilibration

$$\Gamma^{-}_{q_{\ell xy}} \approx \pi^2 54\zeta(3) B^{\not g}_\ell |h_{xx}|^2 T \approx 0.15 \times B^{\not g}_\ell |h_{xx}|^2 T\,, \tag{10}$$

which is valid for $|h_{xx}| \gg |h_{yy}|$ and for the size of the particular lepton Yukawa couplings as in the SM.

2.1.2. *Equations for the flavoured asymmetries*

In deriving Eq. (8), we have accurately taken account of the impact of the gauge and the Yukawa couplings on generating and also damping off-diagonal correlations in $q^{(\mathrm{m})}_\ell$. In the equation represented by Fig. 1(C), the same couplings enter once more. At this level, we adapt from the usual calculations on flavoured Leptogenesis [7,8] the simplifying approximation that flavour correlations in $q^{(\mathrm{f})}_{\ell ab}$ are either unaffected (unflavoured regime) or completely erased (fully flavoured regime). We note that a detailed calculation as for $q^{(\mathrm{m})}_\ell$ should have the result that in the fully flavoured regime, the according components of $q^{(\mathrm{f})}_{\ell ab}$ are suppressed rather than fully erased, what would lead to sub-leading corrections to the present calculations. These flavour effects suggest to distinguish between the following regimes:

A 1 When $2.7 \times 10^{11}\ \mathrm{GeV} \gtrsim T \gtrsim 4.1 \times 10^{10}\ \mathrm{GeV}$, off-diagonal correlations in $q^{(\mathrm{m})}_\ell$ will not have enough time to build up, since $\Gamma^{-}_{q_{\ell\tau\mu}}, \Gamma^{-}_{q_{\ell\tau e}} < H$. Leptogenesis from mixing lepton doublets should therefore be inefficient at these temperatures.

2 For $4.1 \times 10^{10}\ \mathrm{GeV} \gtrsim T \gtrsim 1.3 \times 10^{9}\ \mathrm{GeV}$, the correlations involving τ will build up in $q^{(\mathrm{m})}_\ell$, but $q^{(\mathrm{m})}_{\ell\mu e} = q^{(\mathrm{m})}_{\ell e\mu} \approx 0$ due to $\Gamma^{-}_{q_{\ell\mu e}} \ll H$. Within $q^{(\mathrm{f})}_\ell$, the correlations involving τ are erased due to decohering scattering. In summary, the non-zero entries of the charge-density matrices are given by

$$q^{(\mathrm{m})}_\ell = \begin{pmatrix} 0 & 0 & q^{(\mathrm{m})}_{\ell e\tau} \\ 0 & 0 & q^{(\mathrm{m})}_{\ell\mu\tau} \\ q^{(\mathrm{m})*}_{\ell e\tau} & q^{(\mathrm{m})*}_{\ell\mu\tau} & 0 \end{pmatrix}, \quad q^{(\mathrm{f})}_\ell = \begin{pmatrix} q^{(\mathrm{f})}_{\ell ee} & q^{(\mathrm{f})}_{\ell e\mu} & 0 \\ q^{(\mathrm{f})*}_{\ell e\mu} & q^{(\mathrm{f})}_{\ell\mu\mu} & 0 \\ 0 & 0 & q^{(\mathrm{f})}_{\ell\tau\tau} \end{pmatrix}. \tag{11}$$

B 1 When 1.3×10^9 GeV $\gtrsim T \gtrsim 2.0 \times 10^8$ GeV, the correlations $q^{(\mathrm{m})}_{\ell e\tau}$ and $q^{(\mathrm{m})}_{\ell\mu\tau}$ have enough time to build up, but still not $q^{(\mathrm{m})}_{\ell e\mu}$. All off-diagonal correlations in $q^{(\mathrm{f})}_{\ell}$ decay and should be set to zero due to the direct damping of flavour correlations:

$$q^{(\mathrm{m})}_{\ell} = \begin{pmatrix} 0 & 0 & q^{(\mathrm{m})}_{\ell e\tau} \\ 0 & 0 & q^{(\mathrm{m})}_{\ell\mu\tau} \\ q^{(\mathrm{m})*}_{\ell e\tau} & q^{(\mathrm{m})*}_{\ell\mu\tau} & 0 \end{pmatrix}, \quad q^{(\mathrm{f})}_{\ell} = \begin{pmatrix} q^{(\mathrm{f})}_{\ell ee} & 0 & 0 \\ 0 & q^{(\mathrm{f})}_{\ell\mu\mu} & 0 \\ 0 & 0 & q^{(\mathrm{f})}_{\ell\tau\tau} \end{pmatrix}. \tag{12}$$

2 When $T \lesssim 2.0 \times 10^8$ GeV, all correlations in $q^{(\mathrm{m})}_{\ell}$ have enough time to build up and all off-diagonal correlations in $q^{(\mathrm{f})}_{\ell}$ are erased, such that

$$q^{(\mathrm{m})}_{\ell} = \begin{pmatrix} 0 & q^{(\mathrm{m})}_{\ell e\mu} & q^{(\mathrm{m})}_{\ell e\tau} \\ q^{(\mathrm{m})*}_{\ell e\mu} & 0 & q^{(\mathrm{m})}_{\ell\mu\tau} \\ q^{(\mathrm{m})*}_{\ell e\tau} & q^{(\mathrm{m})*}_{\ell\mu\tau} & 0 \end{pmatrix}, \quad q^{(\mathrm{f})}_{\ell} = \begin{pmatrix} q^{(\mathrm{f})}_{\ell ee} & 0 & 0 \\ 0 & q^{(\mathrm{f})}_{\ell\mu\mu} & 0 \\ 0 & 0 & q^{(\mathrm{f})}_{\ell\tau\tau} \end{pmatrix}. \tag{13}$$

When above constraints on the rates for the creation and for the decay of flavour correlations are not sufficiently saturated, a treatment of incomplete flavour decoherence is in order. This has been put forward in Ref. [9], but it is yet numerically challenging and requires further developments. For the numerical examples presented in this paper, it turns out however that the approximations as described for regime B1 should be appropriate.

In view of these considerations for the generation of flavour correlations, we can now write down the expressions for the matrix Ξ introduced in Eq. (7), that depend on the temperature regime in which Leptogenesis takes place:

$$\Xi = \begin{pmatrix} 1 & 0 & 1 \\ 0 & 1 & 1 \\ 1 & 1 & 1 \end{pmatrix} \text{ in Regimes A2 and B1}, \quad \Xi = \begin{pmatrix} 1 & 1 & 1 \\ 1 & 1 & 1 \\ 1 & 1 & 1 \end{pmatrix} \text{ in Regime B2}. \tag{14}$$

Note that the diagonal components are actually irrelevant, because $\mathcal{Q}_{\ell aa} = 0$.

From above explicit expressions that indicate the non-zero entries of $q^{(\mathrm{m})}_{\ell}$ and $q^{(\mathrm{f})}_{\ell}$, we see that these charge-density matrices are complementary, what justifies the decomposition of the Kadanoff–Baym equations done in Ref. [38], which is represented here in Figs. 1(B) and (C). We should still make a remark though on the fact why we do not consider terms of order Y^2 that multiply $q^{(\mathrm{m},f)}_{\ell}$ on the right-hand side of Fig. 1(B). The reason is that by virtue of the requirement $\Gamma^{-}_{q\ell ab} > H$ for the non-zero correlations $q^{(\mathrm{m})}_{\ell ab}$, the relation $(h^2_{aa} + h^2_{bb})\gamma^{\mathrm{fl}} > H$ should be amply fulfilled as well. Therefore, the flavour damping mediated by the SM Yukawa couplings is more efficient in suppressing the off-diagonal correlations in $q^{(\mathrm{m})}_{\ell ab}$ than the damping induced by the couplings Y, that we therefore neglect. Note however, that in the equation represented by Fig. 1(C), rates of order Y^2 multiply $q^{(\mathrm{f})}_{\ell}$ and $q^{(\mathrm{m})}_{\ell}$. In particular, the second term on the right-hand side is the washout term that suppresses the diagonal charge densities and those of the off-diagonal components, that are unaffected by flavour effects. The second term on the right-hand side is the source term, that we discuss next.

The charge correlations $q^{(\mathrm{m})}_{\ell}$, as given by Eq. (7), are of an out-of-equilibrium form, which can simply be inferred from the fact that they are purely off-diagonal. Therefore, they give rise to a non-vanishing source of correlations for entries of the matrix $q^{(\mathrm{f})}_{\ell}$, which may be diagonal or

non-diagonal. The first term on the right-hand side of Fig. 1(C) is the *CP* violating source that creates flavour asymmetries at the rate[1]

$$\partial_\eta q^{(\mathrm{f})}_{\ell ab} = -\sum_i \frac{3M_{Ni}^{5/2}T^{1/2}}{2^{9/2}\pi^{5/2}} \mathrm{e}^{-\frac{M_{Ni}}{T}} \left(Y^\dagger_{ai} Y_{ic} q^{(\mathrm{m})}_{\ell cb} + q^{(\mathrm{m})}_{\ell ac} Y^\dagger_{ci} Y_{ib} \right) . \tag{15}$$

Note that the flavour structure of this equation takes the anticommutator form present in Eq. (2). When compared with the corresponding result of Ref. [38], we have generalised this source of lepton flavour asymmetries such that it also includes the off-diagonal correlations that are generated and that should be relevant for the regime A2.

2.1.3. Summary of generation of the lepton asymmetry

Aside from the details of the flavour dynamics, we can briefly summarise the present mechanism in terms of the following two steps:

(1) The out-of-equilibrium dynamics of the RHNs induces via the Yukawa couplings Y off-diagonal correlations in the number-densities of active leptons. These are given by $q^{(m)}_{\ell ab}$ as expressed in Eq. (7). Notice that the factor (8) exhibits the well-known form characteristic for resonantly enhanced correlations with damping. It is therefore comparable with the correlations of RHNs in Resonant Leptogenesis [23,24].
(2) Through additional interactions with the RHNs, the off-diagonal correlations act as the source for the flavoured asymmetries as given by Eq. (15).

The main difference with standard Leptogenesis or ARS Leptogenesis is therefore that off-diagonal correlations of the active lepton flavours take over the part of inducing the diagonal asymmetries from the correlations of RHNs.

2.1.4. Relation to density matrix approaches

The equations governing the present scenario of Leptogenesis may alternatively be set up in a density matrix approach. To make this more explicit, we undo the expansion $\delta n^{\pm}_\ell = \delta n^{\pm(\mathrm{m})}_\ell + \delta n^{\pm(\mathrm{f})}_\ell$ and write the kinetic equation derived in the CTP approach that corresponds to Fig. 1(a) as

$$\begin{aligned} &\frac{27\zeta(3)T_{\mathrm{com}}}{\pi^2}\partial_\eta \delta n^{\pm}_\ell \pm \frac{\mathrm{i}}{16}T^2_{\mathrm{com}}[h^2, \delta n^{\pm}_\ell] \\ &\quad = -Y^\dagger B^Y Y \pm \{Y^\dagger S Y, q_\ell\} - B^{\mathrm{fl}}_\ell \{h^2, \delta n^{\pm}_\ell\} \\ &\qquad + 2B^{\mathrm{fl,sca}}_\ell h \delta n^{\pm}_{\mathrm{R}} h - 2B^{\mathrm{fl,ann}}_\ell h \delta n^{\mp}_{\mathrm{R}} h - B^g_\ell (\delta n^+_\ell + \delta n^-_\ell) . \end{aligned} \tag{16}$$

This form of the equation is manifestly flavour-covariant and thereby explicitly exhibits the matrix structure anticipated in Eq. (2). We have introduced for this purpose $B^Y = \mathrm{diag}(B^Y_1, B^Y_2, B^Y_3)$ and S, where the B^Y_i are defined in Eq. (5) and S can be inferred from Eq. (15). In addition, we introduce the number densities $\delta n^{\pm}_{\mathrm{R}}$ of right-handed SM leptons and antileptons, where the flavour structures are derived in Ref. [9]. In order to preserve lepton number conservation in the interactions mediated by h, one should then supplement Eq. (16) with an additional kinetic equation for the right-handed leptons,

[1] We correct here a sign error present in Ref. [38].

$$\frac{27\zeta(3)T_{\rm com}}{\pi^2}\partial_\eta\delta n_{\rm R}^{\pm} = -2B_\ell^{\not\Phi}\{h^2,\delta n_{\rm R}^{\pm}\} + 4B_\ell^{\not\Phi,{\rm sca}}h\delta n_\ell^{\pm}h - 4B_\ell^{\not\Phi,{\rm ann}}h\delta n_\ell^{\mp}h$$
$$- B_{\rm R}^{g}(\delta n_{\rm R}^{+} + \delta n_{\rm R}^{-})\,. \tag{17}$$

In these equations, $B_\ell^{\not\Phi} = B_\ell^{\not\Phi,{\rm sca}} + B_\ell^{\not\Phi,{\rm ann}}$. The quantity $B_\ell^{\not\Phi,{\rm sca}}$ encompasses the rate for scatterings of leptons $\ell + X \leftrightarrow e_{\rm R} + \phi$, where X may stand for a top quark or gauge boson, as well as crossings of X and ϕ and overall charge conjugations. Similarly, $B_\ell^{\not\Phi,{\rm ann}}$ accounts for annihilations of leptons $\ell + \bar{e}_{\rm R} \leftrightarrow X + \phi$ and the charge conjugate processes. According to the term in the equation for left-handed leptons, the equilibration of the right-handed particle and antiparticle densities through pair annihilations is encompassed in Eq. (17) within the term proportional to $B_{\rm R}^g$.

In Eq. (3) the complications of the flavour-covariant formulation above are avoided by restricting the interactions mediated by the SM Yukawa couplings h to the off-diagonal entries of left-handed lepton charges, *i.e.* to the decoherence of correlations. As discussed in Section 2.2, the effect of the diagonal components of the charge density $q_{\rm R} = \delta n_{\rm R}^{+} - \delta n_{\rm R}^{-}$ is accounted for by the usual formalism for spectator effects, while for the dynamics of the off-diagonal correlations in $q_\ell^{({\rm f})}$, we follow the approach pursued in standard treatments of flavoured Leptogenesis [7,8]. In either case, the approximations of Section 2.2 are valid only when the reactions mediated by a particular h_{aa} are either negligible or fully equilibrated.[2] In intermediate regimes, one should indeed use the flavour-covariant formulation given by Eq. (16), implying an increased numerical effort, which is why we do not pursue this possibility in the present work. For flavour effects in standard Leptogenesis, the partial equilibration of the reactions mediated by h is investigated in Ref. [9], whereas for the spectator effects, the partial equilibration is discussed in Ref. [54]. Note that when restricting to the interactions mediated by h, Eqs. (16), (17) can be added to yield $\partial_\eta(2\,q_\ell + q_{\rm R}) = 0$, as a consequence of lepton number conservation in the SM (with the factor two being due to our convention of counting one component of the doublet only within the charge and number densities).

In principle, there are more SM interactions that subsequently (as the Universe cools) become important [54]. Rather than extending the network of kinetic equations by introducing $q_{\rm R}$ and other SM charges, we follow in Section 2.2 the more economical standard procedure of imposing chemical equilibrium constraints, with the disadvantage of losing a manifestly flavour-covariant description.

Now, Eqs. (16), (17) can alternatively be derived in a density-matrix approach, where the commutator terms arise from tree-level masses and hermitian (dispersive) self-energies, while the anticommutators emerge from the absorptive parts of self-energy diagrams, *cf. e.g.* Ref. [45] for the corresponding calculation on Leptogenesis from oscillations of RHNs. Since the equations are formulated in terms of charge densities, the particular rates have to be momentum averaged which enters into the coefficients of the particular terms and introduces a sizeable theoretical uncertainty, *cf.* the discussion in Section 2.1.1.

[2] Note however that for $q_\ell^{({\rm m})}$, in Eqs. (7), (8) we explicitly calculate the off-diagonal correlations even though these are suppressed for the interactions mediated by h being close to equilibrium. On the other hand, $hq_\ell^{({\rm m})}h = 0$, since h is diagonal and $q_\ell^{({\rm m})}$ off-diagonal. It is therefore justified to consider the diagonal entries of $q_{\rm R}$ only, that are induced by $q_\ell^{({\rm f})}$, as done in our treatment of the spectator effects.

The reason for the straightforward agreement between the density-matrix formulation and the CTP approach is due to the fact that the diagrams in Fig. 1(a) are only of one-loop order in terms of resummed propagators, where the relevant resummations are implicitly performed within the solution to the Schwinger–Dyson or density matrix equation, respectively. Therefore, no explicit subtraction of real intermediate states is necessary in the density matrix approach, in contrast density matrix or Boltzmann approaches where decay asymmetries are introduced explicitly into the kinetic equations [12]. Besides, the CTP and the density matrix approaches are the only ones that allow for a reliable description for flavour oscillations in a finite-density medium, and both agree on the overdamping of oscillations of correlations of left-handed leptons [9,10] that is of key relevance for the present scenario.

In this context, we also comment on the expansion $\delta n_\ell^\pm = \delta n_\ell^{\pm(\mathrm{m})} + \delta n_\ell^{\pm(\mathrm{f})}$: While one could numerically integrate the network of Eqs. (16), (17), exploiting hierarchies between the interaction rates allows to reduce the set of kinetic equations that needs to be solved to the one given by Eq. (25a) [with the substitution of Eq. (30)]. The two main simplifications are:

- First, the fact that $\Gamma^-_{q_{\ell ab}}$, which is the damping rate for off-diagonal correlations given in Eq. (9), is much larger than the Hubble rate, allows to neglect time derivatives for the off-diagonal correlations in $q^{(\mathrm{m})}_{\ell ab}$ and therefore to apply the quasi-static expression (7) that only depends on the deviation of the RHNs from equilibrium.
- Second, since $q^{(\mathrm{f})}$ is perturbatively suppressed by an extra order of $Y^\dagger Y$ compared to $q^{(\mathrm{m})}_\ell$ [*cf.* Eq. (15)], we can neglect its effect on the latter quantities.

It is also useful to compare these two points with the case of resonant Leptogenesis in the strong washout regime [24]. When sufficiently far away from the mass-degenerate limit, the time-derivatives in the kinetic equations for the off-diagonal correlations of the RHNs (the quantities corresponding to $q^{(\mathrm{m})}_\ell$) can be neglected (corresponding to the first simplification mentioned above), which is an approximation that is also implied when inserting the loop corrections perturbatively into the decay asymmetry [2,20]. Then, in the decays of the RHNs, there is a helicity asymmetry left behind (as can be seen from the solutions presented in Ref. [20]), that corresponds to $q^{(\mathrm{f})}_\ell$. Since this secondary asymmetry is subdominant, it can be neglected when calculating the subsequent evolution of the off-diagonal correlations of the RHNs (corresponding to the second simplification). While for standard leptogenesis from decays and inverse decays of RHNs, these helicity asymmetries can simply be discarded, the corresponding asymmetries $q^{(\mathrm{f})}_\ell$ are of course the main quantities of interest in the present scenario.

2.1.5. *Comparison with the source term for conventional leptogenesis*

It is of course of interest to compare the asymmetry from lepton mixing with the standard asymmetry from the decays and the mixings of sterile neutrinos. For this purpose, we make use of the standard decay asymmetry including flavour correlations, that is given by [2,9,55]

$$\varepsilon^{Ni}_{ab} = -\frac{3}{16\pi [YY^\dagger]_{ii}} \sum_{j\neq i} \left\{ \mathrm{Im}\left[Y^\dagger_{ai} (Y^* Y^t)_{ij} Y_{jb} \right] \frac{\xi(x_j)}{\sqrt{x_j}} + \mathrm{Im}\left[Y^\dagger_{ai} (YY^\dagger)_{ij} Y_{jb} \right] \frac{2}{3(x_j - 1)} \right\}, \tag{18}$$

where $x_j = (M_{Nj}/M_{Ni})^2$ and

$$\xi(x) = \frac{2}{3}x\left[(1+x)\log\frac{1+x}{x} - \frac{2-x}{1-x}\right]. \tag{19}$$

We should compare the function $\xi(x)$ with $\mathcal{Q}_{\ell ab}$ given in Eq. (8), since both play the role of loop factors, that multiply the *CP* asymmetry that is present in the Yukawa couplings Y. Inspecting $\mathcal{Q}_{\ell ab}$ and ignoring first those of the denominator terms that involve B^{fl}, we observe an enhancement $\sim 1/(h_{aa}^2 - h_{bb}^2)$, which one might naively guess when expecting that the source from lepton mixing is enhanced by the difference of the square of the thermal masses of the leptons. Within $\xi(x_j)$, the corresponding enhancement is explicitly present in the terms $\sim 1/(M_{Ni}^2 - M_{Nj}^2)$. However, within $\mathcal{Q}_{\ell ab}$, the denominator terms that involve B^{fl} indicate that this enhancement is limited by the damping of the flavour correlations, which induce *CP* violation from mixing. We observe two different types of damping: First, the terms $\sim B^{\text{fl}}$ are due to the decoherence of correlations due to scatterings mediated by the SM-lepton Yukawa couplings h. Second, the terms $\sim B^{\text{fl}}B^{g}$ originate from the effect that leptons and anti-leptons oscillate with opposite frequencies. In conjunction with pair creation and annihilation processes, that mediate between leptons and anti-leptons, this leads to flavour decoherence from overdamped oscillations, as it was first described in Ref. [9] and as it is confirmed in Ref. [10]. An appropriate treatment of the resonant limit $x \to 1$ reveals a similar regulating behaviour also for standard Leptogenesis [20–24].

2.2. Flavour correlations and spectator effects

When Leptogenesis occurs at high temperatures, where flavour effects are not important, and when the production and the washout of the asymmetry results from decays and inverse decays of the lightest sterile neutrino, which we call N_1 for now in order to be definite, it is convenient to perform the single-flavour or vanilla approximation. It is based on a unitary flavour transformation (of the left-handed SM leptons) such that N_1 only couples to one linear combination $\ell_\parallel$ of the left-handed leptons. On the other hand, when Leptogenesis occurs at temperatures below 1.3×10^9 GeV, it is advantageous to remain in the basis where the SM Yukawa-couplings h are diagonal. Interactions mediated by these couplings then rapidly destroy off-diagonal flavour correlations. In a practical calculation, we may then just delete the off-diagonal correlations that are induced by the terms (15) and (18) [7,8]. In the range between 1.3×10^9 GeV and 2.7×10^{11} GeV, it is often convenient to perform a two flavour-approximation, where lepton asymmetries are deposited in the flavour τ and in a linear combination σ of e and μ. Correlations between τ and σ are then erased by $h_{\tau\tau}$-mediated interactions. In effect, only diagonal correlations in the flavours τ and σ need to be calculated.

However the reduction to a single flavour at high temperatures or to two uncorrelated flavours between 1.3×10^9 GeV and 2.7×10^{11} GeV only works when N_1 is the only right-handed neutrino that is effectively produced or destroyed in decay and inverse decay processes at times relevant for Leptogenesis, which is typical for hierarchical scenarios where $M_1 \ll M_{2,3}$, and therefore, the heavier of the N_i are strongly Maxwell suppressed. Once more than one of the right-handed neutrinos is effectively produced or destroyed, flavour correlations of the active leptons must be taken into account [10,56], because the combinations $\ell_\parallel$ or σ are in general different for the individual N_i. Now, because for Leptogenesis from mixing lepton doublets, the relevant *CP*-violating cut is purely thermal and it involves a right-handed neutrino that must be different from the decaying neutrino, we must require that there are at least two sterile neutrinos

$N_{1,2}$ with masses $M_{N1,2}$ that are not hierarchical. The latter condition is imposed in order to avoid a Maxwell suppression of the *CP* asymmetry.[3] This implies that for regime A2, we must account for lepton flavour correlations, which in general cannot be avoided by a basis transformation due to the dynamical importance of two sterile neutrinos. In regime B, we may proceed by remaining in the basis where the SM-lepton Yukawa-couplings h are diagonal and simply delete the off-diagonal correlations in the source terms (15) and (18).

In the CTP approach, the collision terms including flavour correlations can be derived in a systematic and straightforward manner. The flavour structure turns out to be in accordance with the anticommutator term in the density matrix equation (2). In order to further improve on the accuracy of the present analysis compared to the one presented in Ref. [38], we include the partial redistribution and equilibration of the flavoured asymmetry within the SM particles present in the plasma, the so-called spectator effects [57–59]. The relevant processes are mediated by Yukawa interactions as well as by the strong and weak sphalerons. It is then useful to track within the Boltzmann equations those asymmetries and correlations for which the diagonal parts are only violated by the decays and the inverse decays of the sterile neutrinos. These are given by

$$\Delta_{aa} = B/3 - L_a\,, \tag{20a}$$

$$\Delta_{ab} = -2q^{(\mathrm{f})}_{\ell ab} \quad \text{for } a \neq b\,, \tag{20b}$$

which we have formulated as a matrix-valued quantity in view of the Boltzmann equations including flavour coherence, that we formulate below. Here, the number density of baryons is given by B, and the diagonal number density of leptons of the flavour a by L_a, *i.e.* it accounts for left- and right-handed SM leptons. In addition to the interactions with sterile neutrinos, the flavour correlations in $q^{(\mathrm{f})}_{\ell}$ are also altered by processes that are mediated by the SM-lepton Yukawa interactions. However, according to our above discussion, we assume that these are either negligible (unflavoured regime) or lead to a complete decoherence (fully flavoured regime). We also note that the quantities denoted by q_X are defined here as the charge densities within a single component of the gauge multiplet X. In contrast, Δ accounts for a the total charge density that is summed over all gauge multiplicities. This implies that if $q_{\ell aa}$ changes by two units, Δ_{aa} does so by minus one.

In order to obtain the washout rates, we must reexpress the $q_{\ell aa}$ in terms of the Δ_{aa}. Moreover, there is also an asymmetry in Higgs bosons that depends on the Δ_{aa}. We obtain these densities through the relations

$$q_{\ell aa} = -\frac{1}{2}\sum_{b\in\{e,\mu,\tau\}} A_{ab}\Delta_{bb}\,, \tag{21a}$$

$$q_{\phi} = \frac{1}{2}\sum_{b\in\{e,\mu,\tau\}} C_{\phi b}\Delta_{bb}\,. \tag{21b}$$

As explained above, the redistribution of the asymmetries due to the spectators only afflicts the diagonal components of q_ℓ. For regime A, we take strong sphalerons, weak sphalerons (that couple to the trace of q_ℓ), interactions mediated by Yukawa couplings of the t, b, c quarks and τ leptons to be in equilibrium. This leads to

[3] This can be seen when substituting Eq. (5) into Eq. (15) and noting that the non-vanishing terms always involve two different N_i along with their distribution functions.

$$A = \frac{1}{589}\begin{pmatrix} -503 & 86 & 60 \\ 86 & -503 & 60 \\ 30 & 30 & -390 \end{pmatrix}, \tag{22a}$$

$$C_\phi = -\frac{1}{589}\begin{pmatrix} 164 & 164 & 216 \end{pmatrix}. \tag{22b}$$

In regime B, the τ-lepton and s-quark mediated interactions equilibrate in addition, what leaves us with

$$A = \frac{1}{1074}\begin{pmatrix} -906 & 120 & 120 \\ 75 & -688 & 28 \\ 75 & 28 & -688 \end{pmatrix}, \tag{23a}$$

$$C_\phi = -\frac{1}{179}\begin{pmatrix} 37 & 52 & 52 \end{pmatrix}. \tag{23b}$$

Note that the factors of $1/2$ in Eqs. (21) are due to SU(2) doublet nature of ℓ and ϕ and to our convention of $q_{\ell aa}$ and q_ϕ to account for one component of the SU(2) doublet only.

2.3. Boltzmann equations

With above explanations and remarks, and with the calculational details given in Ref. [38], we put together Boltzmann equations that describe the freeze-out of the lepton asymmetry. In contrast to the most commonly studied scenarios, we now have more than one sterile neutrino in the game. Therefore, we distinguish the asymmetries that are created through the decays and inverse decays of the individual N_i as $q_\ell^{(\mathrm{m},f)Ni}$ and Δ^{Ni}, such that Eq. (7) is decomposed as

$$q_{\ell ab}^{(\mathrm{m})Ni} = \frac{\mathcal{Q}_{ab}}{T^2} Y_{ai}^\dagger Y_{ib} B_i^Y . \tag{24}$$

Furthermore, we follow the common procedure of expressing the Boltzmann equations in terms of the ratios $Y_{Ni} = n_{Ni}/s$, $Y_\ell^{Ni} = q_\ell^{(\mathrm{f})Ni}/s$, $Y_\phi^{Ni} = q_\phi^{Ni}/s$ and $Y_\Delta^{Ni} = \Delta^{Ni}/s$, where s denotes the entropy density.

It is convenient to parametrise the time evolution through variables $z_i = M_{Ni}/T$, in terms of which the equations that describe the freeze-out of the asymmetry can be expressed in the following approximate form:

$$\frac{dY_\Delta^{Ni}}{dz_i} = -2\bar{S}_\ell^{Ni}(Y_{Ni} - Y_{Ni}^{\mathrm{eq}}) - \bar{W}_\Delta[Y_\Delta^{Ni}], \tag{25a}$$

$$\frac{dY_{Nk}}{dz_i} = \bar{C}_{Nk}(Y_{Nk} - Y_{Nk}^{\mathrm{eq}}), \tag{25b}$$

where Y_{Ni}^{eq} is the equilibrium value of Y_{Ni}. Through Eqs. (5), (6), (7), (15), we can identify the source term for Leptogenesis from mixing leptons

$$\bar{S}_{\ell ab}^{Ni} = -\Lambda_{ab} \sum_{\substack{j\neq i \\ jc}} \frac{3a_{\mathrm{R}} z_i^{\frac{9}{2}} \mathrm{e}^{-\frac{M_{Nj}}{M_{Ni}} z_i}}{2^{23/2}\pi^{7/2}} \frac{M_{Nj}^{\frac{7}{2}}}{M_{Ni}^{\frac{9}{2}}} \frac{[YY^\dagger]_{ii}}{[YY^\dagger]_{jj}} \mathrm{i} \times \left(\mathcal{Q}_{\ell cb} Y_{ai}^\dagger Y_{ic} Y_{cj}^\dagger Y_{jb} + \mathcal{Q}_{\ell ac} Y_{aj}^\dagger Y_{jc} Y_{ci}^\dagger Y_{ib} \right). \tag{26}$$

In the diagrammatic representation, this source corresponds to the first term on the right-hand side of Fig. 1(C). According to what we state above regarding the effect of the SM lepton–Yukawa couplings, we should choose

$$\Lambda = \begin{pmatrix} \Lambda_{ee} & \Lambda_{e\mu} & \Lambda_{e\tau} \\ \Lambda_{\mu e} & \Lambda_{\mu\mu} & \Lambda_{\mu\tau} \\ \Lambda_{\tau e} & \Lambda_{\tau\mu} & \Lambda_{\tau\tau} \end{pmatrix} = \begin{pmatrix} 1 & 1 & 0 \\ 1 & 1 & 0 \\ 0 & 0 & 1 \end{pmatrix} \quad \text{in Regime A}\,, \tag{27a}$$

$$\Lambda = \begin{pmatrix} 1 & 0 & 0 \\ 0 & 1 & 0 \\ 0 & 0 & 1 \end{pmatrix} \quad \text{in Regime B}\,, \tag{27b}$$

such that correlations that are suppressed by Yukawa-mediated interactions faster than the Hubble rate are deleted from the outset. We re-emphasise that a transformation to an effective two-flavour basis is not possible in Regime A when more than one of the sterile neutrinos is involved in the washout [10,56].

The Boltzmann equations (25) apply to standard Leptogenesis as well. In that case, the source is given by

$$\bar{S}^{Ni}_{\ell ab} = \Lambda_{ab} \frac{1}{2} \bar{\mathcal{C}}_{Ni} \varepsilon^{Ni}_{ab}\,. \tag{28}$$

We have defined here the $\bar{S}_{\ell ab}$ in Eqs. (26), (28) such that these comply for $a = b$ with the expressions given in Ref. [38], where these are introduced as a source for q_ℓ rather than Δ. The various factors $-1/2$ and -2 therefore account for the ℓ being SU(2) doublets.

At this point, it is of interest to compare the decay asymmetry (18) for standard Leptogenesis with the source term (26) for the present scenario. The first contribution to Eq. (18) arises from lepton-number violating amplitudes (involving the chirality flip of a sterile neutrino), whereas the second contribution is due to lepton-number conserving but lepton-flavour violating diagrams. When comparing this latter term with Eq. (26), we observe the same structure of Yukawa couplings Y, but with different weights due to the involvement of the SM Yukawa couplings h (via $\mathcal{Q}_\ell$) in the suppression of the off-diagonal flavour correlations of the left-handed leptons. The similarity is of course a consequence of the fact that the processes which are of importance for generating the initial asymmetries for the present mechanism are lepton-number conserving as well. In Ref. [38], additional details on this point are given. In particular, the off-diagonal correlations $q^{\mathrm{m}}_{\ell ab}$ do not only give rise to a source term for lepton flavour asymmetries, but also for helicity asymmetries within the RHNs. It can be shown that the sum over the sources of all asymmetries within the left-handed SM leptons and the RHNs is zero, which is a useful consistency check. Since we are in the strong washout regime, despite the helicity asymmetry, the non-relativistic RHNs decay at leading order without leaving behind a lepton asymmetry. Notably, this is different for relativistic RHNs, where a helicity asymmetry approximately corresponds to a chirality asymmetry, and therefore asymmetries can be conserved within that sector for comparably long times, which is of importance for the details of Leptogenesis from oscillations of RHNs [20,36,45–49].

The decay rate of the sterile neutrino N_k in terms of the variable z_i is

$$\bar{\mathcal{C}}_{Nk} = \frac{1}{8\pi} \sum_a Y_{ka} Y^\dagger_{ak} a_{\mathrm{R}} z_i \frac{M_{Nk}}{M^2_{Ni}}\,. \tag{29}$$

In the non-relativistic approximation, this agrees with its thermal average up to relative corrections of order T/M_{Nk}. In the strong washout regime, a substantial simplification arises from

the fact that the deviation of the sterile neutrinos from equilibrium is small, such that we can approximate

$$(Y_{Nk} - Y_{Nk}^{\rm eq}) \approx \frac{1}{\bar{\mathcal{C}}_{Nk}} \frac{dY_{Nk}^{\rm eq}}{dz_i} \,. \tag{30}$$

We use this relation for both scenarios, Leptogenesis from mixing leptons as well as from the decay and mixing of sterile neutrinos. The error incurred through this standard approximation is investigated in Refs. [30,50].

Finally, we need to obtain an expression for the washout rate $\bar{W}[Y_\ell^{Ni}]$, that is of the anticommutator form indicated in the density matrix equation (2) and that should account for the spectator effects. In terms of Feynman diagrams, the washout term corresponds to the second graph on the right-hand side of Fig. 1(C). As explained above, washout affects the flavour-diagonal lepton charges and the off diagonal correlations in a different manner, such that it is useful to define

$$Y_\Delta^{\rm diag} = {\rm diag}\left(Y_{\Delta ee}, Y_{\Delta\mu\mu}, Y_{\Delta\tau\tau}\right) , \tag{31a}$$

$$\vec{Y}_\Delta = \left(Y_{\Delta ee}, Y_{\Delta\mu\mu}, Y_{\Delta\tau\tau}\right)^t , \tag{31b}$$

$$Y_\Delta^{\rm wo} = Y_\Delta - Y_\Delta^{\rm diag} + {\rm diag}\left(A\,\vec{Y}_\Delta\right) , \tag{31c}$$

where the superscript t indicates a transposition. The matrix components of the washout rate are given by

$$\mathcal{B}_{\ell ab}^{Ni,k} = Y_{ak}^\dagger Y_{kb} \frac{3}{2^{7/2}\pi^{5/2}} \left(\frac{M_{Nk}}{M_{Ni}}\right)^{\frac{5}{2}} \frac{a_{\rm R}}{M_{Ni}} z_i^{\frac{5}{2}} {\rm e}^{-z_i \frac{M_{Nk}}{M_{Ni}}} \,. \tag{32}$$

Putting together the washout terms induced by lepton and by Higgs charge densities, we eventually obtain for the washout term

$$\bar{W}_\Delta[Y_\Delta] = \sum_k \left(\frac{1}{2}\{\mathcal{B}_\ell^{Ni,k}, Y_\Delta^{\rm wo}\} + \frac{1}{2}\mathcal{B}_\ell^{Ni,k}(1,1,1)^t[C_\phi \vec{Y}_\Delta]\right) . \tag{33}$$

The factor of $1/2$ in front of the Higgs-induced term can be understood when noting that $q_\ell = \mu_\ell T^2/6$, whereas $q_\phi = \mu_\phi T^2/3$, where $\mu_{\ell,\phi}$ are chemical potentials and the factor two is due to the difference between Fermi and Bose statistics.

3. Parametric surveys

3.1. Parametrisation of the Yukawa couplings

Taking diagonal matrices for the sterile neutrino masses M_N, the neutrino sector of the model (1) yet encompasses 18 parameters: 3 sterile neutrino masses and 15 parameters in the Yukawa coupling Y. (While the complex 3×3 matrix Y has eighteen degrees of freedom, three of these can be absorbed by phase rotations of the SM leptons ℓ.) This large number of parameters is a typical obstacle to comprehensive studies of the parameter space in type-I see-saw models.

The Casas–Ibarra parametrisation [60] facilitates to impose the observational constraints from neutrino oscillations by rearranging the Lagrangian parameters into low and high energy categories. The nine high energy parameters are given by $M_{N1,2,3}$ as well as three complex angles ϱ_{12}, ϱ_{13}, ϱ_{23}, in terms of which one defines the complex orthogonal matrix

$$\mathcal{R} = \begin{pmatrix} c_{12}c_{13} & c_{13}s_{12} & s_{13} \\ -c_{23}s_{12} - c_{12}s_{23}s_{13} & c_{23}s_{12} - s_{12}s_{23}s_{13} & c_{13}s_{23} \\ s_{12}s_{23} - c_{12}c_{23}s_{13} & -c_{12}s_{23} - c_{23}s_{12}s_{13} & c_{13}c_{23} \end{pmatrix}, \tag{34}$$

where $s_{ij} = \sin\varrho_{ij}$ and $c_{ij} = \cos\varrho_{ij}$.

The nine low-energy parameters are given in terms of the diagonal mass-matrix of the active neutrinos $m_\nu = \mathrm{diag}(m_1, m_2, m_3)$ and the six real angles and phases of the PMNS matrix

$$U_\nu = V^{(23)} U_\delta V^{(13)} U_{-\delta} V^{(12)} \,\mathrm{diag}(e^{i\alpha_1/2}, e^{i\alpha/2}, 1)\,, \tag{35}$$

where

$$V^{(12)} = \begin{pmatrix} \cos\vartheta_{12} & \sin\vartheta_{12} & 0 \\ -\sin\vartheta_{12} & \cos\vartheta_{12} & 0 \\ 0 & 0 & 1 \end{pmatrix}, \quad V^{(13)} = \begin{pmatrix} \cos\vartheta_{13} & 0 & \sin\vartheta_{13} \\ 0 & 1 & 0 \\ -\sin\vartheta_{13} & 0 & \cos\vartheta_{13} \end{pmatrix}, \tag{36}$$

$$V^{(23)} = \begin{pmatrix} 1 & 0 & 0 \\ 0 & \cos\vartheta_{23} & \sin\vartheta_{23} \\ 0 & -\sin\vartheta_{23} & \cos\vartheta_{23} \end{pmatrix},$$

and $U_{\pm\delta} = \mathrm{diag}(e^{\mp i\delta/2}, 1, e^{\pm i\delta/2})$. In terms of this parametrisation, the Yukawa couplings of the sterile neutrinos are obtained as

$$Y^\dagger = U_\nu \sqrt{m_\nu}\mathcal{R}\sqrt{M_N}\frac{\sqrt{2}}{v}\,. \tag{37}$$

A considerable, yet generic simplification occurs when one of the three sterile neutrinos decouples, say N_3 for definiteness. This can happen when the Yukawa couplings Y_{3a} are very small, when M_3 is very large or when we only assume the existence of two sterile neutrinos to start with. Note that such a configuration requires one of the light neutrinos to be massless. If we therefore take $m_1 = 0$, we imply that

$$\varrho_{23} = 0 \quad \varrho_{13} = \pi/2\,. \tag{38}$$

Moreover, the Yukawa couplings as given by Eq. (37) then turn out to be independent of α_1, as an immediate consequence of $m_1 = 0$.

Altogether, in the decoupling scenario, there are 11 Lagrangian parameters (9 parameters in the Yukawa couplings Y after rephasings and two Majorana masses for the sterile neutrinos). These decompose into 4 high energy parameters ($M_{N1,2}$ and ϱ_{12}) and 7 low-energy parameters (m_2, m_3, three angles ϑ_{ij} and the two phases δ and α_2). Out of the latter, 5 have been measured experimentally (Δm^2, $\delta m^2 \approx m_2^2$ and the three PMNS mixing angles ϑ_{ij}). The free parameters of the model are therefore $M_{N1,2}$, ϱ, α and δ, while for the PMNS mixing angles in our numerical examples, we choose $\sin\vartheta_{12} = 0.55$, $\sin\vartheta_{23} = 0.63$ and $\sin\vartheta_{13} = 0.16$, which are close to the best-fit values determined by current observations [61,62].

3.2. The parameter space in the decoupling scenario

The production rates of the N_i, the washout rates of the asymmetries as well as the *CP* cuts entering the production rates of the lepton asymmetries that are presented in Section 2 apply all to the non-relativistic regime, *i.e.* when $M_{Ni} \gg T$ for all N_i that are involved in a certain rate. In order to employ these results consistently, we should then avoid situations when at times relevant for the freeze-out value of the asymmetry relativistic N_i are present. For the purpose of the

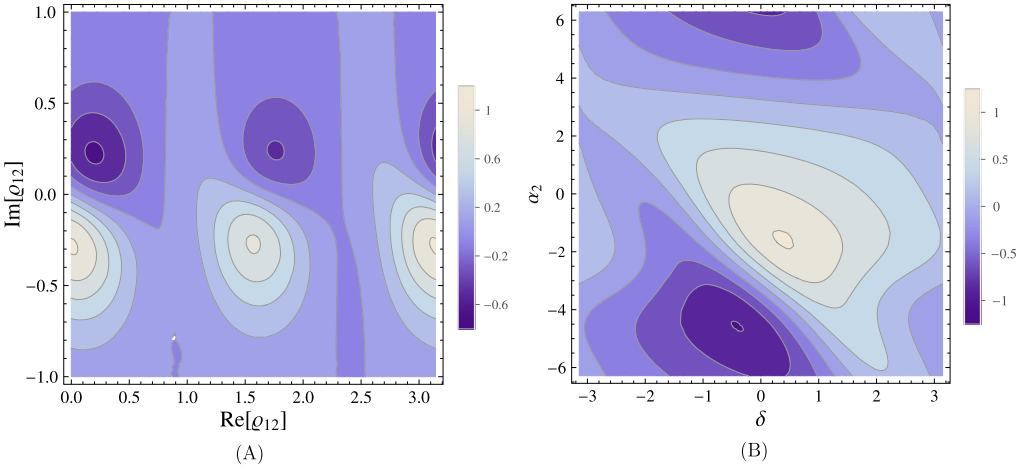

Fig. 2. Asymmetry $Y/Y_{\rm obs}$ in the ϱ_{12} plane (A) and in the δ–α_2 plane (B), with the remaining parameters as specified in Table 1.

Table 1
Set of parameters that yields the largest asymmetry for Leptogenesis from mixing lepton doublets in the decoupling scenario (effectively two RHNs only).

M_{N1}	3.67×10^9 GeV	m_1	0 meV	α_2	-1.7
M_{N2}	3.2×10^9 GeV	m_2	8.7 meV	δ	0.4
		m_3	49 meV	ϱ_{12}	$0.02-0.31$i

present analysis, we therefore choose RHN masses that are not hierarchical, while not necessarily degenerate. Besides, for the source from mixing SM leptons, such parametric configurations are also favoured by the fact that the asymmetry from the decay of the lightest of the N_i is exponentially suppressed in the case of hierarchical M_i, *cf.* Eq. (26) above and Fig. 4 below. In future work, it may be of interest though to consider relativistic RHNs when the asymmetry does not result from the decay of the lightest RHN, as certain flavour correlations may generically survive the washout from the lighter RHNs [56,63,64].

Now, as we observe below, the dependence of the final asymmetry on the relative size of M_1 and M_2 turns out to be mild (*cf.* Fig. 4). Besides, given the relation (37) and the Boltzmann equations from Section 2.3, we see that the value of the freeze-out asymmetry scales proportional to the M_{Ni} when keeping the mass ratios fixed. Therefore, a scan over the four-dimensional parameter space defined by ϱ_{12}, δ and α_2 yields comprehensive information on the model in the decoupling scenario [with ϱ_{23} and ϱ_{13} as in Eqs. (38)], given the constraints mentioned above. For the purpose of the scan, we choose the masses of the two RHNs as these are given in Table 1. The remaining values specified in Table 1 correspond to the point that we find in parameter space for which the maximal asymmetry occurs. We use the flavour approximations as specified for Regime B 1 in Section 2.1.2.

In Fig. 2, we show the freeze-out asymmetry

$$Y = \sum_{a,i} Y^{Ni}_{\Delta aa}(z_i \to \infty) \tag{39}$$

normalised to the observed baryon-minus-lepton asymmetry [65,66]

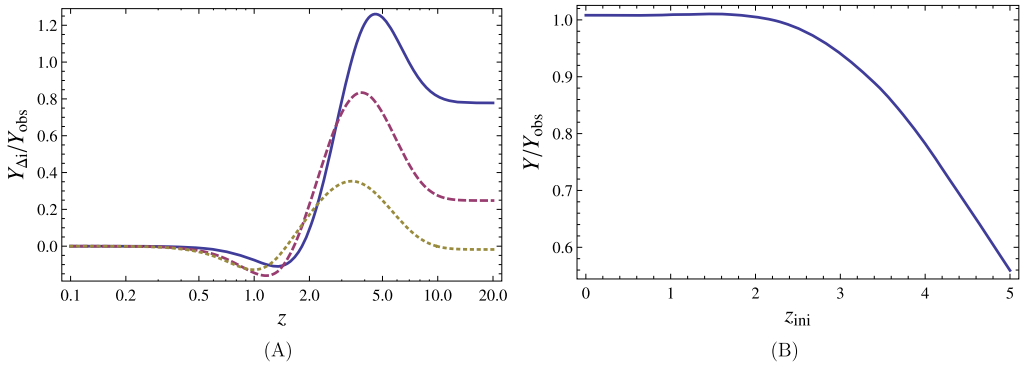

Fig. 3. In panel (A), we show the evolution of the asymmetries $Y_{\Delta i}$ with $i = e, \mu, \tau$ (solid blue, dashed red, dotted yellow) normalised to $Y_{\rm obs}$ over z. In panel (B), we show the value of the freeze-out asymmetry (sum over three flavours) over $z_{\rm ini}$. The parameters are given in Table 1. (For interpretation of the references to color in this figure legend, the reader is referred to the web version of this article.)

$$Y_{\rm obs} = \left(\frac{28}{79}\right)^{-1} \times 8.6 \times 10^{-11}\,, \tag{40}$$

where the first factor accounts for the conversion to the final baryon asymmetry via sphalerons [67]. We vary parameters in the planes ϱ_{12} and δ *vs.* α_2, where we fix the remaining parameters as in Table 1. The alignment of some of the contours along $\delta + \frac{\alpha}{2} = \text{const.}$ in Fig. 2(B) can be attributed to a constant washout of the e-flavour, since we find for the Yukawa couplings that (*cf.* Refs. [49,68])

$$Y_{1e} = \frac{\sqrt{2M_1}}{v}\left(-e^{i\frac{\alpha}{2}}\sqrt{m_2}\cos\vartheta_{13}\sin\vartheta_{12}\sin\varrho_{12} - e^{-i\delta}\sqrt{m_3}\sin\vartheta_{13}\cos\varrho_{12}\right), \tag{41a}$$

$$Y_{2e} = \frac{\sqrt{2M_2}}{v}\left(e^{i\frac{\alpha}{2}}\sqrt{m_2}\cos\vartheta_{13}\sin\vartheta_{12}\cos\varrho_{12} - e^{i\delta}\sqrt{m_3}\sin\vartheta_{13}\sin\varrho_{12}\right). \tag{41b}$$

Next, we validate the assumption of strong washout and non-relativistic RHNs by considering the evolution of the individual flavour asymmetries $Y_{\Delta i} = Y^{N1}_{\Delta ii} + Y^{N2}_{\Delta ii}$ over the parameter $z = M_{N1}/T$, that is commonly used as the time variable when studying Leptogenesis from massive neutrinos. From Fig. 3 (A), we observe that, as it is typical for strong washout scenarios, the freeze-out value of the asymmetry settles when $z \gtrsim 10$. In order to assess further the validity of the non-relativistic approximation for the RHNs as well as in order to determine the minimum value of the required reheat temperature, we start the integration of the Boltzmann equations at some value $z = z_{\rm ini}$ with vanishing asymmetries as boundary conditions (while for all other numerical results, we start the integration at $z = z_{\rm ini} = 0$). From Fig. 3 (B) we see that the result changes by less than 10% as long as $z_{\rm ini} \lesssim 3$. This independence of the details of the initial evolution of the asymmetries is a typical feature of the strong washout regime. Given the value of M_{N1} from Table 1, we may therefore conclude that the minimum required reheat temperature $T_{\rm reh}$ in the decoupling scenario is $T_{\rm reh} \gtrsim 1.2 \times 10^9\,\text{GeV}$. Due to the order one uncertainties incurred through the estimate of B^g_ℓ and the momentum averaging leading to B^{fl}_ℓ, this should be considered as coincident with the bound of $T_{\rm reh} \gtrsim 2 \times 10^9\,\text{GeV}$ for standard Leptogenesis [59, 69,70]. However, the present optimal (by the criterion of minimising the lower bound on $T_{\rm reh}$) point given in Table 1 is clearly distinct from the optimal parametric configurations in standard

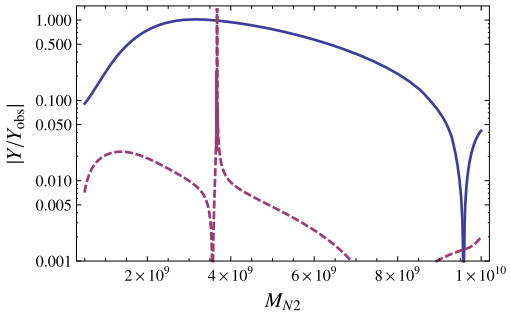

Fig. 4. Dependence of the freeze-out asymmetry from lepton mixing on the parameter M_{N2}, with the remaining parameters as specified in Table 1 (solid blue). For comparison, we show the asymmetry from standard Leptogenesis for the same parameters (dashed red). (For interpretation of the references to color in this figure legend, the reader is referred to the web version of this article.)

Table 2
Parametric example point for the scenario with three RHNs.

M_{N1}	3×10^8 GeV	m_1	2.5 meV	α_1	0.4	ϱ_{12}	$0.01+0.05$i
M_{N2}	4×10^8 GeV	m_2	9.1 meV	α_2	0.2	ϱ_{23}	$-0.19-0.19$i
M_{N3}	5×10^8 GeV	m_3	49 meV	δ	1.1	ϱ_{13}	$2.1+3.0$i

Leptogenesis because here, we are in the strong washout regime, while for the standard source, the lowest viable reheat temperatures occur in between the strong and the weak washout regimes.

The analysis presented in Fig. 3 (B) also justifies the use of the flavour approximations for Regime B 1, valid for temperatures roughly below 1.3×10^9 GeV. While in fact, for $z\lesssim3$, Our scenario falls into Regime A 2, the final prediction for the asymmetry should not be substantially affected by an inaccurate treatment of the flavour effects at early times.

Finally, we vary M_{N2} while keeping the remaining parameters fixed as in Table 1. The resulting normalised freeze-out asymmetry is shown in Fig. 4. We thus indeed verify that the ratio of M_{N1} to M_{N2} has no dramatic influence on the freeze-out asymmetry as long it remains of order *one*. For comparison, we also show in Fig. 4 the asymmetry that arises for the same parameters from standard Leptogenesis. While we clearly see the resonance for $M_{N2}\to M_{N1}$, away from this narrow enhanced region, the result is small compared to the asymmetry arising from lepton mixing. One should note however that there exist parametric configurations that are more favourable for standard Leptogenesis, in particular when saturating the bound on the reheat temperature from Refs. [59,69,70].

3.3. Three sterile neutrinos

Adding a third RHN N_3 implies that compared to the case with two RHNs only, the resulting asymmetry depends in addition on M_{N3}, α_1, ϱ_{23}, ϱ_{13} and the absolute mass scale of the light neutrinos, *i.e.* there are seven extra parameters. This appears to prohibit a comprehensive analysis of the parameter space in practice. Nonetheless, it is interesting to evaluate the asymmetries for an example point, that would be consistent with a smaller reheat temperature. We discuss how an enhanced asymmetry becomes possible even if generated at lower temperatures and how parameters need to be tweaked in order to arrange for such a situation.

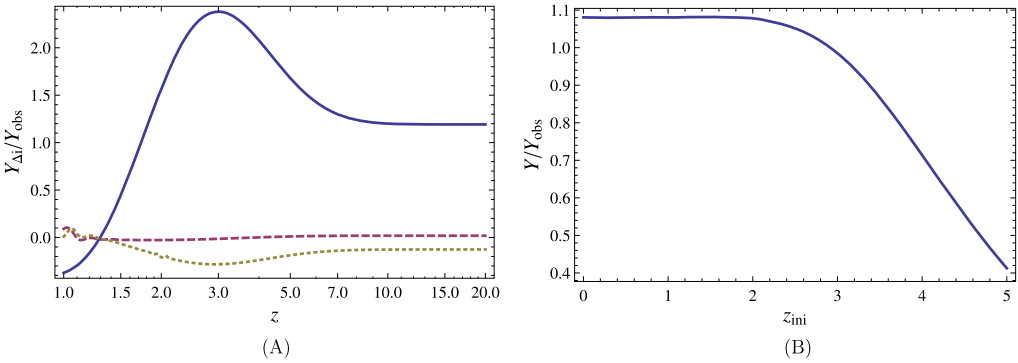

Fig. 5. In panel (A), we show the evolution of the asymmetries $Y_{\Delta i}$ with $i = e, \mu, \tau$ (solid blue, dashed red, dotted yellow) normalised to $Y_{\rm obs}$ over z. In panel (B), we show the value of the freeze-out asymmetry (sum over three flavours) over $z_{\rm ini}$. The parameters are given in Table 2. (For interpretation of the references to color in this figure legend, the reader is referred to the web version of this article.)

In Table 2, we present the point in parameter space for which we determine the freeze-out lepton asymmetry, where it can be seen from Fig. 5 that an asymmetry in accordance with the observed value is obtained. Moreover, as exhibited in Fig. 5(A), the final asymmetry is dominated by the e-flavour. This can be understood by an inspection of the matrix of Yukawa couplings that satisfies $|Y_{ie}| \ll |Y_{i\mu}|, |Y_{i\tau}|$, such that there is a substantially smaller washout rate for ℓ_e than for ℓ_μ and ℓ_τ. On the other hand, larger $Y_{i\mu}$ and $Y_{i\tau}$ enhance the asymmetry $q_{\ell ee}$, *cf.* Eq. (15).

Turning to the parameters in Table 2, we observe the large imaginary part for ϱ_{13}, which implies that the Yukawa couplings have a larger magnitude than for configurations with smaller imaginary parts of the ϱ_{ij}. This implies that there is a cancellation in individual terms contributing to the masses of the light neutrinos in the see-saw mechanism, which may be interpreted as parametric tuning. It is noteworthy that situations with large couplings of $\ell_{\mu,\tau}$ and relatively small couplings of ℓ_e to the RHNs are also favoured in scenarios of Leptogenesis where the *CP*-violating source arises from the oscillations of relativistic RHNs [35,36,49,64,71] (the so-called ARS scenarios, after the authors of Ref. [36]). We emphasise that however, the source from active lepton mixing is different from the source from RHN oscillations, and while the favoured parametric configurations bear similarities in the pattern of Yukawa couplings, for given masses of the RHNs, the main contributions to the asymmetries are generated in both scenarios at very different temperatures, *cf.* Ref. [64].

4. Conclusions

In this work, we have investigated in some detail the possibility of generating the baryon asymmetry of the Universe from the mixing of lepton doublets within the SM extended by two or three RHNs. For this purpose, we have introduced a diagrammatic representation of the underlying mechanism, and we have discussed the dynamics of the flavour correlations of SM leptons at various temperatures. We then have performed a comprehensive parametric study in the setup with two RHNs in the type-I see-saw mechanism. For the case with three RHNs, we have identified a way to achieve lower reheat temperatures that are consistent with the observed baryon asymmetry.

We find that baryogenesis from mixing lepton doublets is a generically viable scenario in the type-I see-saw framework, provided

- there are RHNs present in the mass range between 10^9 GeV and 10^{11} GeV (*cf.* the discussion of Section 2.1.1 concerning the upper bound and the numerical findings of Section 3 regarding the lower bound)
- and these RHNs are of the same mass-scale, while they do not need to be degenerate.

The lower mass bound on the RHNs and consequently on the reheat temperature can be evaded through a certain alignment of the Yukawa couplings Y, that allows these to be relatively large while the masses of the light active neutrinos remain small, which is possible in the presence of three RHNs, *cf.* Section 3.3.

Methodically, the present calculation draws from formulations of Leptogenesis in the CTP approach that have been applied to the resonant regime [20], to oscillations of relativistic RHNs [35] as well as to the decoherence of active lepton flavours [9]. To this end, we identify the quantities $B_\ell^{\not\Phi}$ and B_ℓ^{g} as the main contributors to the theoretical uncertainty. In introducing these, we average over the lepton momentum-modes under the simplifying assumption of identical reaction rates. While such a procedure is common practice in similar calculations for Leptogenesis from oscillations of RHNs (*cf. e.g.* Ref. [35,45,48]), it would nonetheless be desirable to improve on this approximation in the future by resolving the different reaction rates for each momentum mode.

It is interesting to observe that the minimal reheat temperatures for standard Leptogenesis and for baryogenesis from mixing lepton doublets appear to coincide. For couplings as in the SM, the term $(h_{aa}^2 + h_{bb}^2) B_\ell^{\not\Phi} B_\ell^{g}$ in the enhancement factor, Eq. (8), numerically dominates in the denominator. Smaller gauge couplings would therefore lead to a larger asymmetry. On the other hand, the size of the gauge couplings does not have a leading influence on the asymmetry for standard Leptogenesis [59,69,70]. Therefore, the similar bound on the reheat temperatures can be attributed to a parametric coincidence.

We also note that the analysis in the present study is valid for the strong washout regime, *i.e.* the situation where the RHNs can be approximated as non-relativistic during the creation of the asymmetry. It would be interesting to relax this assumption (which should be possible for at least one of the RHNs when three or more RHNs are present altogether) because one may then anticipate substantially larger deviations from equilibrium. In that case, a calculation would however not enjoy the considerable simplifications that arise from treating the RHNs as non-relativistic.

While we have considered here the somewhat minimal framework of the SM augmented by RHNs, our analysis implies that new gauged particles that share the same quantum numbers and that are nearly degenerate or effectively become degenerate at higher temperatures are generic candidates for being involved in creating the matter–antimatter asymmetry. This opens new prospects for scenarios of baryogenesis from out-of-equilibrium reactions in the expanding Universe.

Acknowledgements

We acknowledge support by the Gottfried Wilhelm Leibniz programme of the Deutsche Forschungsgemeinschaft (DFG) and by the DFG cluster of excellence ‘Origin and Structure of the Universe’.

Appendix A. Cut contribution to lepton self-energy

The presence of cuts in self-energy diagrams is required in conjunction with phases in the Lagrangian in order to obtain *CP*-violating phenomena. Furthermore, the all-important washout rate can be interpreted as the cut that corresponds to lepton absorption within the plasma. While it is calculationally advantageous to directly convolute the cuts with phase-space integrals weighted by the pertinent distribution functions, as we do in the main part of our calculations, we isolate in the following the cuts relevant for *CP* violation and washout for illustrative purposes.

Within finite-density environments, cut contributions are given by the Wightman-type self-energies, where for positive (negative) energies, the $<$ ($>$) variant corresponds to the production rate and the $>$ ($<$) variant to the absorption rate within the background. This can be seen when considering the Kadanoff–Baym equation for the doublet leptons in its form that is obtained after an integration over four momentum [30,38]:

$$\frac{d}{d\eta}q_{\ell ab} = \frac{1}{2}\int \frac{d^4k}{(2\pi)^4}\mathrm{tr}\left[\{\mathrm{i}\not{\Sigma}^{>}_{\ell}(k), \mathrm{i}S^{<}_{\ell}(k)\} - \{\mathrm{i}\not{\Sigma}^{<}_{\ell}(k), \mathrm{i}S^{>}_{\ell}(k)\}\right]_{ab}, \tag{A.1}$$

where curly brackets denote anticommutators in lepton-flavour space. For $M_{Ni} \gtrsim T$, the leading contribution to the lepton self-energy is given by [30]

$$\mathrm{i}\not{\Sigma}^{<,>}_{\ell ab}(k) = \sum_i Y^{\dagger}_{ai}Y_{ib}\int \frac{d^4p}{(2\pi)^4}\frac{d^4q}{(2\pi)^4}(2\pi)^4\delta^{(4)}(k-p-q)P_{\mathrm{R}}\mathrm{i}S^{<,>}_{Ni}(p)P_{\mathrm{L}}\mathrm{i}\Delta^{>,<}_{\phi}(-q)\,. \tag{A.2}$$

The tree-level, non-equilibrium propagators $\mathrm{i}S_{\ell}$, $\mathrm{i}\Delta_{\phi}$, $\mathrm{i}S_N$ for the lepton doublet, Higgs doublet and the RHN are given in Ref. [30].

For the purpose of the present work, it is often advantageous to substitute the above form for $\mathrm{i}\not{\Sigma}^{<,>}_{\ell}$ under the integral in Eq. (A.1) and then to make use of cancellations within the integrand that are based on the Kubo–Martin–Schwinger (KMS) relations, rather than calculating $\mathrm{i}\not{\Sigma}^{<,>}_{\ell}$ explicitly. In particular, one should consider the deviation of the lepton and Higgs doublets from equilibrium as small perturbations, which leads to considerable simplifications of the integrand that can be used in order to derive the quantities B^{Y}_{i} (the relation of which to Eq. (A.1) can be directly inferred from Ref. [38]), relevant for the generation of off-diagonal flavour correlations, or $\bar{W}_{\Delta}$, relevant for washout.

In order to show that the cut-contributions are sizeable within the thermal background while these clearly vanish at zero temperature, we now evaluate $\mathrm{tr}[\mathrm{i}\not{k}\mathrm{i}\not{\Sigma}^{<,>}_{\ell}]$. This Dirac trace is the only form in which the thermal cuts enter into the source and washout terms for the present mechanism of Leptogenesis as well as for standard scenarios [30]. We therefore calculate

$$\mathrm{tr}[\mathrm{i}\not{k}\mathrm{i}\not{\Sigma}^{<,>}_{\ell}]_{ab}\Big|_{k^0=|\mathbf{k}|} = \sum_i Y^{\dagger}_{ai}Y_{ib}\frac{M^2_{Ni}}{8\pi|\mathbf{k}|}\int\limits_{\frac{M^2_{Ni}}{4|\mathbf{k}|}}^{\infty} d|\mathbf{q}|\mathcal{F}^{<,>}_i(|\mathbf{k}|+|\mathbf{q}|,|\mathbf{q}|)\,, \tag{A.3}$$

where

$$\begin{aligned}\mathcal{F}^{<}_i(E_1,E_2) &= -f_{Ni}(E_1)(1+f_{\phi}(E_2))\,,\\ \mathcal{F}^{>}_i(E_1,E_2) &= (1-f_{Ni}(E_1))f_{\phi}(E_2)\,,\end{aligned} \tag{A.4}$$

and f_{Ni}, f_ϕ are the distributions of the RHNs and Higgs doublets as functions of energy. As one should expect, the lepton production rate vanishes for a zero RHN-distribution, whereas there is no absorption for a vanishing Higgs distribution.

Since we assume strong washout ($M_{Ni} \gg T$), we then can approximate the distributions of RHNs and Higgs doublets to be of the Maxwell form with a pseudo chemical potential μ_{Ni} and a proper chemical potential μ_ϕ

$$f_{Ni}(|\mathbf{k}|+|\mathbf{q}|) = \mathrm{e}^{-(|\mathbf{k}|+|\mathbf{q}|-\mu_{Ni})/T}\,, \qquad f_\phi(|\mathbf{q}|) = \mathrm{e}^{-(|\mathbf{q}|-\mu_\phi)/T}\,. \tag{A.5}$$

Within the strong washout approximation, we only need to evaluate those contributions with a single exponential factor in the integrand, such that

$$\mathrm{tr}[i\not{k}\not{\Sigma}^<_\ell]_{ab}\Big|_{k^0=|\mathbf{k}|} = -\sum_i Y^\dagger_{ai} Y_{ib} \frac{M^2_{Ni} T}{8\pi |\mathbf{k}|} \mathrm{e}^{-(|\mathbf{k}|+M^2_{Ni}/(4|\mathbf{k}|)-\mu_{Ni})/T}\,, \tag{A.6a}$$

$$\mathrm{tr}[i\not{k}\not{\Sigma}^>_\ell]_{ab}\Big|_{k^0=|\mathbf{k}|} = \sum_i Y^\dagger_{ai} Y_{ib} \frac{M^2_{Ni} T}{8\pi |\mathbf{k}|} \mathrm{e}^{-(M^2_{Ni}/(4|\mathbf{k}|)-\mu_\phi)/T}\,. \tag{A.6b}$$

For $\mu_{Ni} = 0$ and $\mu_\phi = 0$, we recognise the KMS relation $\not{\Sigma}^>_\ell(k) = -\mathrm{e}^{k^0}\not{\Sigma}^<_\ell(k)$. The cuts for negative k^0 follow when exchanging $k^0 \to -k^0$, $\{<,>\} \to \{>,<\}$, $\mu_\phi \to -\mu_\phi$ and $\mu_{Ni} \to \mu_{Ni}$ within this result.

In the strong washout regime, radiative corrections to these cuts, most notably due to gauge couplings, top-quark Yuakwa interactions and self-interactions of the Higgs boson are perturbatively suppressed, as it has been confirmed in Refs. [72–74] that are concerned with the production rate of non-relativistic RHNs. A systematic calculation of the radiative corrections to the *CP*-violating rates is still missing, as explicitly concluded in Ref. [75], but we may expect that these are perturbatively suppressed compared to the leading rates used in this work. The situation is different for the ARS scenario [20,36,45–49], where the RHNs are mainly produced in $2 \leftrightarrow 2$ scatterings and $1 \leftrightarrow 2$ decays $\phi \to \ell + N_i$ (that open kinematically due to the top-loop dominated thermal mass of the Higgs boson) because the $1 \leftrightarrow 2$ processes with tree-level masses that dominate for strong washout are kinematically suppressed for ultrarelativistic RHNs ($M_{Ni} \ll T$). The *CP*-violating cuts that implicitly or explicitly enter calculations on ARS Leptogenesis can therefore be interpreted as being partly associated with the production of extra gauge bosons or top quarks.

References

[1] See, e.g. Chapters 12 and 13 of J. Beringer, et al., Particle Data Group Collaboration, Review of particle physics (RPP), Phys. Rev. D 86 (2012) 010001.

[2] L. Covi, E. Roulet, F. Vissani, CP violating decays in leptogenesis scenarios, Phys. Lett. B 384 (1996) 169, arXiv:hep-ph/9605319.

[3] M. Flanz, E.A. Paschos, U. Sarkar, J. Weiss, Baryogenesis through mixing of heavy Majorana neutrinos, Phys. Lett. B 389 (1996) 693, arXiv:hep-ph/9607310.

[4] A. Pilaftsis, Resonant CP violation induced by particle mixing in transition amplitudes, Nucl. Phys. B 504 (1997) 61, arXiv:hep-ph/9702393.

[5] A. Pilaftsis, CP violation and baryogenesis due to heavy Majorana neutrinos, Phys. Rev. D 56 (1997) 5431, arXiv:hep-ph/9707235.

[6] T. Endoh, T. Morozumi, Z.-h. Xiong, Primordial lepton family asymmetries in seesaw model, Prog. Theor. Phys. 111 (2004) 123, arXiv:hep-ph/0308276.

[7] A. Abada, S. Davidson, F.X. Josse-Michaux, M. Losada, A. Riotto, Flavour issues in leptogenesis, J. Cosmol. Astropart. Phys. 0604 (2006) 004, arXiv:hep-ph/0601083.

[8] E. Nardi, Y. Nir, E. Roulet, J. Racker, The importance of flavor in leptogenesis, J. High Energy Phys. 0601 (2006) 164, arXiv:hep-ph/0601084.
[9] M. Beneke, B. Garbrecht, C. Fidler, M. Herranen, P. Schwaller, Flavoured leptogenesis in the CTP formalism, Nucl. Phys. B 843 (2011) 177, arXiv:1007.4783 [hep-ph].
[10] S. Blanchet, P. Di Bari, D.A. Jones, L. Marzola, Leptogenesis with heavy neutrino flavours: from density matrix to Boltzmann equations, J. Cosmol. Astropart. Phys. 1301 (2013) 041, arXiv:1112.4528 [hep-ph].
[11] M. Fukugita, T. Yanagida, Baryogenesis without grand unification, Phys. Lett. B 174 (1986) 45.
[12] E.W. Kolb, S. Wolfram, Baryon number generation in the early universe, Nucl. Phys. B 172 (1980) 224; E.W. Kolb, S. Wolfram, Nucl. Phys. B 195 (1982) 542 (Erratum).
[13] J.S. Schwinger, Brownian motion of a quantum oscillator, J. Math. Phys. 2 (1961) 407.
[14] L.V. Keldysh, Diagram technique for nonequilibrium processes, Zh. Eksp. Teor. Fiz. 47 (1964) 1515, Sov. Phys. JETP 20 (1965) 1018.
[15] E. Calzetta, B.L. Hu, Nonequilibrium quantum fields: closed time path effective action, Wigner function and Boltzmann equation, Phys. Rev. D 37 (1988) 2878.
[16] T. Prokopec, M.G. Schmidt, S. Weinstock, Transport equations for chiral fermions to order $\hbar$ and electroweak baryogenesis. Part 1, Ann. Phys. 314 (2004) 208, arXiv:hep-ph/0312110.
[17] T. Prokopec, M.G. Schmidt, S. Weinstock, Transport equations for chiral fermions to order $\hbar$ and electroweak baryogenesis. Part II, Ann. Phys. 314 (2004) 267, arXiv:hep-ph/0406140.
[18] A. De Simone, A. Riotto, Quantum Boltzmann equations and leptogenesis, J. Cosmol. Astropart. Phys. 0708 (2007) 002, arXiv:hep-ph/0703175.
[19] M. Garny, A. Hohenegger, A. Kartavtsev, M. Lindner, Systematic approach to leptogenesis in nonequilibrium QFT: self-energy contribution to the CP-violating parameter, Phys. Rev. D 81 (2010) 085027, arXiv:0911.4122 [hep-ph].
[20] B. Garbrecht, M. Herranen, Effective theory of resonant leptogenesis in the closed-time-path approach, Nucl. Phys. B 861 (2012) 17, arXiv:1112.5954 [hep-ph].
[21] M. Garny, A. Kartavtsev, A. Hohenegger, Leptogenesis from first principles in the resonant regime, Ann. Phys. 328 (2013) 26, arXiv:1112.6428 [hep-ph].
[22] S. Iso, K. Shimada, M. Yamanaka, Kadanoff–Baym approach to the thermal resonant leptogenesis, J. High Energy Phys. 1404 (2014) 062, arXiv:1312.7680 [hep-ph].
[23] S. Iso, K. Shimada, Coherent flavour oscillation and CP violating parameter in thermal resonant leptogenesis, J. High Energy Phys. 1408 (2014) 043, arXiv:1404.4816 [hep-ph].
[24] B. Garbrecht, F. Gautier, J. Klaric, Strong washout approximation to resonant leptogenesis, J. Cosmol. Astropart. Phys. 1409 (2014) 09, 033, arXiv:1406.4190 [hep-ph].
[25] A. Hohenegger, A. Kartavtsev, Leptogenesis in crossing and runaway regimes, J. High Energy Phys. 1407 (2014) 130, arXiv:1404.5309 [hep-ph].
[26] W. Buchmuller, S. Fredenhagen, Quantum mechanics of baryogenesis, Phys. Lett. B 483 (2000) 217, arXiv:hep-ph/0004145.
[27] M. Garny, A. Hohenegger, A. Kartavtsev, M. Lindner, Systematic approach to leptogenesis in nonequilibrium QFT: vertex contribution to the CP-violating parameter, Phys. Rev. D 80 (2009) 125027, arXiv:0909.1559 [hep-ph].
[28] A. Anisimov, W. Buchmüller, M. Drewes, S. Mendizabal, Leptogenesis from quantum interference in a thermal bath, Phys. Rev. Lett. 104 (2010) 121102, arXiv:1001.3856 [hep-ph].
[29] M. Garny, A. Hohenegger, A. Kartavtsev, Medium corrections to the CP-violating parameter in leptogenesis, Phys. Rev. D 81 (2010) 085028, arXiv:1002.0331 [hep-ph].
[30] M. Beneke, B. Garbrecht, M. Herranen, P. Schwaller, Finite number density corrections to leptogenesis, Nucl. Phys. B 838 (2010) 1, arXiv:1002.1326 [hep-ph].
[31] B. Garbrecht, Leptogenesis: the other cuts, Nucl. Phys. B 847 (2011) 350–366, arXiv:1011.3122 [hep-ph].
[32] A. Anisimov, W. Buchmuller, M. Drewes, S. Mendizabal, Quantum leptogenesis I, Ann. Phys. 326 (2011) 1998, arXiv:1012.5821 [hep-ph].
[33] P.S. Bhupal Dev, P. Millington, A. Pilaftsis, D. Teresi, Flavour covariant transport equations: an application to resonant leptogenesis, Nucl. Phys. B 886 (2014) 569, arXiv:1404.1003 [hep-ph].
[34] P.S.B. Dev, P. Millington, A. Pilaftsis, D. Teresi, Kadanoff–Baym approach to flavour mixing and oscillations in resonant leptogenesis, arXiv:1410.6434 [hep-ph].
[35] M. Drewes, B. Garbrecht, Leptogenesis from a GeV seesaw without mass degeneracy, J. High Energy Phys. 1303 (2013) 096, arXiv:1206.5537 [hep-ph].
[36] E.K. Akhmedov, V.A. Rubakov, A.Y. Smirnov, Baryogenesis via neutrino oscillations, Phys. Rev. Lett. 81 (1998) 1359, arXiv:hep-ph/9803255.
[37] B. Garbrecht, Leptogenesis from additional Higgs doublets, Phys. Rev. D 85 (2012) 123509, arXiv:1201.5126 [hep-ph].

[38] B. Garbrecht, Baryogenesis from mixing of lepton doublets, Nucl. Phys. B 868 (2013) 557, arXiv:1210.0553 [hep-ph].
[39] A.D. Dolgov, Neutrinos in the early universe, Sov. J. Nucl. Phys. 33 (1981) 700, Yad. Fiz. 33 (1981) 1309.
[40] R. Barbieri, A. Dolgov, Neutrino oscillations in the early universe, Nucl. Phys. B 349 (1991) 743.
[41] K. Enqvist, K. Kainulainen, J. Maalampi, Refraction and oscillations of neutrinos in the early universe, Nucl. Phys. B 349 (1991) 754.
[42] K. Enqvist, K. Kainulainen, M.J. Thomson, Stringent cosmological bounds on inert neutrino mixing, Nucl. Phys. B 373 (1992) 498.
[43] G. Sigl, G. Raffelt, General kinetic description of relativistic mixed neutrinos, Nucl. Phys. B 406 (1993) 423.
[44] B. Garbrecht, F. Glowna, P. Schwaller, Scattering rates for leptogenesis: damping of lepton flavour coherence and production of singlet neutrinos, Nucl. Phys. B 877 (2013) 1, arXiv:1303.5498 [hep-ph].
[45] T. Asaka, M. Shaposhnikov, The nuMSM, dark matter and baryon asymmetry of the universe, Phys. Lett. B 620 (2005) 17, arXiv:hep-ph/0505013.
[46] L. Canetti, M. Drewes, M. Shaposhnikov, Sterile neutrinos as the origin of dark and baryonic matter, Phys. Rev. Lett. 110 (6) (2013) 061801, arXiv:1204.3902 [hep-ph].
[47] L. Canetti, M. Drewes, T. Frossard, M. Shaposhnikov, Dark matter, baryogenesis and neutrino oscillations from right handed neutrinos, arXiv:1208.4607 [hep-ph].
[48] T. Asaka, S. Eijima, H. Ishida, Kinetic equations for baryogenesis via sterile neutrino oscillation, J. Cosmol. Astropart. Phys. 1202 (2012) 021, arXiv:1112.5565 [hep-ph].
[49] B. Shuve, I. Yavin, Baryogenesis through neutrino oscillations: a unified perspective, Phys. Rev. D 89 (2014) 075014, arXiv:1401.2459 [hep-ph].
[50] A. Basboll, S. Hannestad, Decay of heavy Majorana neutrinos using the full Boltzmann equation including its implications for leptogenesis, J. Cosmol. Astropart. Phys. 0701 (2007) 003, arXiv:hep-ph/0609025.
[51] J.M. Cline, K. Kainulainen, K.A. Olive, Protecting the primordial baryon asymmetry from erasure by sphalerons, Phys. Rev. D 49 (1994) 6394, arXiv:hep-ph/9401208.
[52] A. Anisimov, D. Besak, D. Bödeker, Thermal production of relativistic Majorana neutrinos: strong enhancement by multiple soft scattering, J. Cosmol. Astropart. Phys. 1103 (2011) 042, arXiv:1012.3784 [hep-ph].
[53] D. Besak, D. Bödeker, Thermal production of ultrarelativistic right-handed neutrinos: complete leading-order results, J. Cosmol. Astropart. Phys. 1203 (2012) 029, arXiv:1202.1288 [hep-ph].
[54] B. Garbrecht, P. Schwaller, Spectator effects during leptogenesis in the strong washout regime, J. Cosmol. Astropart. Phys. 1410 (10) (2014) 012, arXiv:1404.2915 [hep-ph].
[55] S. Antusch, P. Di Bari, D.A. Jones, S.F. King, Leptogenesis in the two right-handed neutrino model revisited, Phys. Rev. D 86 (2012) 023516, arXiv:1107.6002 [hep-ph].
[56] S. Antusch, P. Di Bari, D.A. Jones, S.F. King, A fuller flavour treatment of N_2-dominated leptogenesis, Nucl. Phys. B 856 (2012) 180, arXiv:1003.5132 [hep-ph].
[57] R. Barbieri, P. Creminelli, A. Strumia, N. Tetradis, Baryogenesis through leptogenesis, Nucl. Phys. B 575 (2000) 61, arXiv:hep-ph/9911315.
[58] W. Buchmüller, M. Plümacher, Spectator processes and baryogenesis, Phys. Lett. B 511 (2001) 74, arXiv:hep-ph/0104189.
[59] S. Davidson, E. Nardi, Y. Nir, Leptogenesis, Phys. Rep. 466 (2008) 105, arXiv:0802.2962 [hep-ph].
[60] J.A. Casas, A. Ibarra, Oscillating neutrinos and $\mu \to e, \gamma$, Nucl. Phys. B 618 (2001) 171, arXiv:hep-ph/0103065.
[61] G.L. Fogli, E. Lisi, A. Marrone, D. Montanino, A. Palazzo, A.M. Rotunno, Global analysis of neutrino masses, mixings and phases: entering the era of leptonic CP violation searches, Phys. Rev. D 86 (2012) 013012, arXiv:1205.5254 [hep-ph].
[62] D.V. Forero, M. Tortola, J.W.F. Valle, Global status of neutrino oscillation parameters after Neutrino-2012, Phys. Rev. D 86 (2012) 073012, arXiv:1205.4018 [hep-ph].
[63] P. Di Bari, Seesaw geometry and leptogenesis, Nucl. Phys. B 727 (2005) 318, arXiv:hep-ph/0502082.
[64] B. Garbrecht, More viable parameter space for leptogenesis, Phys. Rev. D 90 (2014) 063522, arXiv:1401.3278 [hep-ph].
[65] G. Hinshaw, et al., WMAP Collaboration, Nine-year Wilkinson Microwave Anisotropy Probe (WMAP) observations: cosmological parameter results, Astrophys. J. Suppl. Ser. 208 (2013) 19, arXiv:1212.5226 [astro-ph.CO].
[66] P.A.R. Ade, et al., Planck Collaboration, Planck 2013 results. XVI. Cosmological parameters, Astron. Astrophys. (2014), arXiv:1303.5076 [astro-ph.CO].
[67] J.A. Harvey, M.S. Turner, Cosmological baryon and lepton number in the presence of electroweak fermion number violation, Phys. Rev. D 42 (1990) 3344.
[68] T. Asaka, S. Eijima, H. Ishida, Mixing of active and sterile neutrinos, J. High Energy Phys. 1104 (2011) 011, arXiv:1101.1382 [hep-ph].

[69] S. Davidson, A. Ibarra, A lower bound on the right-handed neutrino mass from leptogenesis, Phys. Lett. B 535 (2002) 25, arXiv:hep-ph/0202239.
[70] W. Buchmuller, P. Di Bari, M. Plumacher, Leptogenesis for pedestrians, Ann. Phys. 315 (2005) 305, arXiv:hep-ph/0401240.
[71] L. Canetti, M. Drewes, B. Garbrecht, Lab-to-Genesis, arXiv:1404.7114 [hep-ph].
[72] A. Salvio, P. Lodone, A. Strumia, Towards leptogenesis at NLO: the right-handed neutrino interaction rate, J. High Energy Phys. 1108 (2011) 116, arXiv:1106.2814 [hep-ph].
[73] M. Laine, Y. Schroder, Thermal right-handed neutrino production rate in the non-relativistic regime, J. High Energy Phys. 1202 (2012) 068, arXiv:1112.1205 [hep-ph].
[74] S. Biondini, N. Brambilla, M.A. Escobedo, A. Vairo, An effective field theory for non-relativistic Majorana neutrinos, J. High Energy Phys. 1312 (2013) 028, arXiv:1307.7680.
[75] D. Bodeker, M. Sangel, Order g^2 susceptibilities in the symmetric phase of the Standard Model, arXiv:1501.03151 [hep-ph].